EFFECTS OF HYDROSTRATIGRAPHY AND BASIN DEVELOPMENT ON HYDRODYNAMICS OF THE PALO DURO BASIN, TEXAS

by
R. K. Senger,
G. E. Fogg,
and
C. W. Kreitler

Bureau of Economic Geology
W. L. Fisher, Director
The University of Texas at Austin
University Station, Box X
Austin, Texas 78713

1985

DRAFT

EFFECTS OF HYDROSTRATIGRAPHY AND BASIN DEVELOPMENT ON HYDRODYNAMICS OF THE PALO DURO BASIN, TEXAS

ABSTRACT

INTRODUCTION

Scope
Mechanisms for Underpressuring

HYDROGEOLOGY

Geologic Setting
Physiography and Climate
Recharge and Discharge

DATA BASE

Hydraulic Head and Pressure
Hydraulic Properties
    Ogallala Formation
    Dockum Group
    Permian Evaporite Strata
    San Andres Carbonate
    Lower Permian Pennsylvanian Strata
    Salt Dissolution Zone
Specific Storage

COMPUTER PROGRAMS

MODELING PROCEDURE

Finite Element Mesh
Boundary Conditions

LIMITATION OF THE MODEL

SIMULATION STRATEGY: STEADY-STATE MODEL

RESULTS AND DISCUSSION

Effect of Hydrostratigraphy
    Granite-wash Permeability
        1. Simulation A-1
        2. Simulation A-2
        3. Simulation A-3
    Role of Evaporite aquitard
        1. Simulation B-1
        2. Simulation B-2
        3. Simulation B-3
    Interconnection of Ogallala and Dockum Aquifers
        Simulation C
    Effect of Pecos River

DRAFT

ABSTRACT

A two-dimensional ground-water flow model was constructed along a cross section through the Palo Duro Basin to characterize regional ground-water flow paths, and to investigate causes of the underpressuring below the Evaporite aquitard and mechanisms of recharge and discharge to and from the Deep-Basin Brine aquifer. Various effects of lithostratigraphy and topography on ground-water flow were investigated using steady-state flow simulations. Further, the changes in regional hydrodynamics caused by different tectonic and geomorphologic processes were described using transient flow simulations.

The regional ground-water flow pattern in the Palo Duro Basin can be characterized by a shallow ground-water flow system governed primarily by topography, and a deeper flow regime recharging in the New Mexico area and passing deep beneath the Pecos River into the deep section of the Palo Duro Basin. The Evaporite aquitard effectively separates the deeper flow regime from the more rapidly circulating shallow aquifer system, although leakage through the aquitard is important and could contribute up to 27 percent of water passing through the deep section. The ground-water flow pattern within the Deep-Basin Brine aquifer is strongly controlled by the spatial distribution of more permeable strata such as the granite-wash deposits which act to drain the deep aquifer system with greater ease than it is recharged.

Repeated simulations with the model demonstrate that chief causes of underpressuring are the regional topography and geology. Specifically, the Ogallala water table is relatively high due to the elevation of the High Plains; the potentiometric surface of the Deep-Basin Brine aquifer is relatively low due to the draining effect of permeable granite wash strata and very low recharge rates; and the low-permeability Evaporite aquitard effectively segregates the two aquifer systems, thereby maintaining the large head differential. The Pecos River serves as a discharge area of some of the ground water from the west that would otherwise move downdip into the deep aquifers; thus, capture of recharge water enhances underpressuring in the deep section beneath the western half of the High Plains.

1

DRAFT

Simulations of the hydrodynamic development of the Palo Duro Basin as a result of successive tectonic and geomorphologic events indicates that Cenozoic uplift and tilting of the Basin (10 to 15 m. y.) resulted in significant increase in ground-water velocity field. The timing of the erosional events implies that significant underpressuring (head difference between shallow and deep aquifers in excess of 175 m) occurred within the last one to two million years as a result of the caprock retreat. The drastic change of hydraulic heads during that period suggests a significant effect on the overall ground-water flow pattern in the deep section within the last one to two million years.

The modeling effort also indicated that erosional unloading in connection with the retreat of the Caprock Escarpment is ineffective in creating large-scale underpressuring in the Deep-Basin Brine aquifer. Only in the vicinity of the escarpment is it possible that erosional unloading and the resulting expansion of the underlying aquitard could create significant subhydrostatic conditions within the shallow aquitard section. Similarly, hydrocarbon production and the concomitant reduction in reservoir pressure affect hydraulic heads only locally and do not influence the regional ground-water flow in the Deep-Basin Brine aquifer.

DRAFT

INTRODUCTION

Information on the regional hydrogeology of the Palo Duro Basin is important in the investigation of the suitability of this basin for high-level nuclear waste disposal. Predictions of the long-term behavior of a nuclear waste repository require detailed knowledge and understanding of ground-water hydrology in the region surrounding the site. Transportation by ground water is the most likely mechanism by which radionuclides could reach the biosphere from an underground repository.

The Permian Evaporite aquitard, the potential host strata for a waste site, is underlain by the Deep-Basin Brine aquifer which is composed of Wolfcampian, Pennsylvanian, and Pre-Pennsylvanian strata (table 1). The Deep-Basin Brine aquifer is underpressured with respect to water table conditions in the Ogallala aquifer overlying the Evaporite aquitard in the center of the basin. That is, hydraulic head in the Deep-Basin Brine aquifer is much lower than hydraulic head in the Ogallala aquifer. Orr and Kreitler (1985) investigated pressure-depth data from the deep brine aquifers in the Palo Duro Basin and distinguished the observed sub-hydrostatic pressures as being the result of regionally underpressured conditions and apparent under-pressured conditions. According to their definition "apparently underpressured" referred to the shift of pressure-depth trend toward lower pressures solely by topographic effects, and "underpressured" referred to the shift of pressure-depth trend toward lower pressure by an amount greater than could be attributed to topographic effects (Orr and Kreitler, 1985). The plot of pressure versus depth (fig. 1) indicating underpressured conditions shows that fluid pressures in the deep aquifer are lower, by as much as 6.89 MPa (1,000 psi), than brine hydrostatic pressures. This corresponds to a decrease of hydraulic heads by as much as 700 m (2,300 ft) from the Ogallala to the bottom of the Evaporite aquitard. The head difference suggests that (1) permeability of the aquitard is very low and the Ogallala-Dockum aquifer is consequently isolated from the deeper aquifer system, and (2) if contaminants did escape from a repository site within the Evaporite aquitard, they would move downward rather than upward.

3

DRAFT

Characterization of the regional flow regime in the Palo Duro Basin has been assisted by numerical ground-water flow models as described by INTERA (1984), Senger and Fogg (1983), and Wirojanagud and others (1984). In general, the models incorporate available hydrogeologic information and simulate hydraulic head distribution and fluxes under steady-state conditions assuming uniform temperature and density of the fluid. The computed hydraulic heads and fluxes are then compared to available data in order to evaluate the adequacy of the conceptual model.

The conceptualized flow regime in the Palo Duro Basin is generally assumed to represent a steady-state, gravity-driven flow system of the type described by Hubbert (1940). Ground-water flow is governed by the fluid potential along the topographic surface and permeability of the hydrostratigraphic units. While topography controls the regional hydraulic gradient, which, in the Palo Duro Basin, is generally from west to east, the potentiometric surfaces in the deep aquifers indicate ground-water flow to the northeast toward relatively permeable arkosic fan deposits along the Amarillo Uplift (Smith and others, 1985).

In the Palo Duro Basin, extensive modification of the topography as a result of tectonic and geomorphologic processes has occurred within the last 15 million years (McGookey, 1984; Gustavson and others, 1981). Therefore, hydraulic heads observed in the Deep-Basin Brine aquifer may be in transient state and are still responding to modifications of topography in the past; thus, the observed underpressuring may be the result of transient flow conditions.

Extensive hydrocarbon production in the East Texas oil and gas fields has been found to cause significant pressure reduction in the Woodbine Formation (Bell and Shephard, 1951). Similarly, the observed reservoir-pressure decline from production of oil and gas fields in the Texas Panhandle may cause transient underpressured conditions.

4

DRAFT

Scope

A two-dimensional ground-water flow model was constructed along a cross section through the Palo Duro Basin to characterize regional ground-water flow paths as well as to investigate causes of the underpressuring below the Evaporite aquitard and mechanisms of recharge and discharge to and from the Deep-Basin Brine aquifer. The objective of this study is primarily to investigate various factors affecting the overall ground-water flow pattern in the basin, and is not necessarily aimed at producing a fully calibrated predictive model.

In the first phase, the model simulates steady-state ground-water flow conditions using (1) data on hydraulic conductivity from various hydrologic units in the section and (2) hydraulic head and recharge rates along the boundaries of the model. In the second phase, long-term transient flow conditions caused by different tectonic and geomorphologic processes are investigated through the use of time varying boundary conditions. The hydrodynamic development of the basin is crucial to the origin and hydrochemical evolution of the fluids in the deep basin. Changing hydraulic head distributions with time results in changes in ground-water flow paths and in residence time of waters in the basin. Consequently, transport of chemical constituents could have traveled along ancient pathways much different than is suggested by the present-day hydraulic head distribution observed in the basin. In addition, transient modeling is used to investigate other possible effects on the system such as erosional unloading and extensive hydrocarbon production.

Mechanisms for Underpressuring

A variety of mechanisms causing underpressuring in deep-basin aquifers have been suggested by a number of investigators which include (1) epeirogenetic movements, (2) erosion with associated effects on temperature and dilation, (3) piracy of streams, (4) draining through relatively permeable formations, and (5) presence of large oil and gas fields.

DRAFT

Epeirogenetic movements such as uplift and tilting of a basin could significantly alter pressure distributions (Bradely, 1975). Examples are shown in figure 2a for a confined aquifer which pinches out further downdip. If the system is tilted away from the outcrop, thereby elevating hydraulic head in the recharge area, pressures will increase and hydraulic head may rise far above land surface. If the system is tilted in the opposite direction, thereby lowering the outcrop enough to make it a discharge area, fluid drains from the aquifer more easily than can be recharged; consequently underpressured conditions result (fig. 2a).

Erosion of sediments with accompanied lowering of the water table causes the inherited fluid pressure within a sealed formation at depth to become abnormally high (fig. 2b, top), whereas deposition with an increase in the shallow water table causes the inherited fluid pressure within a sealed formation at depth to become abnormally low, compared to hydrostatic pressure conditions (fig. 2b, bottom). Thermal and compactional effects causing possible excess fluid pressures are not considered in this idealized example.

Large-scale erosion which generally accompanies uplift and tilting of a basin can also cause underpressuring by both temperature decrease of the fluids and dilation of low permeable strata that are capable of expanding. Bradely (1975) showed that for a given temperature reduction, pore fluid volume will be reduced more than the pore volume and overall fluid pressures will decrease.

Neuzil and Pollock (1983) investigated the dilation of shales caused by erosional unloading. A decrease of overburden pressure results in an increase in pore volume and a concomitant decrease of fluid pressure in "tight" formations. The combined effects of temperature decrease and overburden removal have been suggested to cause underpressuring in hydrocarbon reservoirs in the Appalachian region (Russel, 1972) and in the Alberta Basin (Dickey and Cox, 1977). Ferran (1973) explained regional underpressuring in Morrow sandstone in the Anadarko Basin by "decompressional expansion" and associated temperature reduction. According to his interpretation, underpressuring in the largely incompressible sandstone formation is caused by pore-pressure change due to temperature reduction and due to the fluid movement from the

6

DRAFT

sandstones into the adjacent shales which expanded in pore volume as a result of overburden stress reduction (fig. 3).

Tóth (1978) documented the importance of topographic relief on general ground-water flow pattern. Tóth and Millar (1983) investigated the origin and maintenance of abnormal fluid pressures as a result of delayed adjustment of subsurface pore pressures to erosional modifications of topography. Their results indicated that it is possible for subareal erosion to generate pore-pressure changes at great depths by cross-formational energy transfer. Tóth and Millar (1983) also showed that fluid pressures at great depths may be in transient state for hundreds to millions of years responding to changes in topography in the past.

Similarly, deposition and a concomitant increase in water-table elevation can cause underpressuring in the deep formation where observed hydraulic heads are in transient state and have not yet equilibrated to the higher water table (fig. 2b). On the other hand, stream valley erosion and the corresponding drop in water-table elevation can significantly modify the regional ground-water flow system resulting in underpressuring caused by the capture of recharge water that would otherwise move downdip into the deep section.

Fertl (1976) proposed a scenario similar to the one shown in the lower diagram of figure 2a to explain underpressuring in the Panhandle oil and gas field in northwest Texas. The permeable granite-wash producing formation crops out to the east in the Wichita Mountains of Oklahoma at an elevation of about 305 m (1,000 ft) above sea level which corresponds approximately to the potentiometric surface of the producing formation in the Panhandle oil and gas field (Fertl, 1976).

Subnormal formation pressures can also occur artificially by large scale production of hydrocarbon reservoirs if no strong water drive occurs to compensate for the pressure decline (Fertl, 1976). For example, significant decline of regional fluid pressures has been observed in the Woodbine formation as a result of extensive hydrocarbon production in the East Texas oil and gas field (Bell and Shephard, 1951). In the Panhandle oil and gas field, which is located at

7

DRAFT

the northeastern boundary of the Palo Duro Basin, reservoir pressures dropped as much as 2.76 MPa (400 psi) since the start of hydrocarbon production in the early 1940's.

Law and Dickinson (1985) developed a conceptual model for abnormally pressured gas accumulations in low-permeability reservoirs. In general, they infer that underpressured conditions originate from previously overpressured gas reservoirs that existed during the early compactional stage of the basin, whereby relatively high temperatures resulted in relatively higher rates of gas accumulation as compared to updip gas loss. Underpressured reservoirs are characterized by a reverse relation whereby gas losses exceed gas generation downdip (Law and Dickinson, 1985). This occurs during a later stage of basin development characterized by uplift and erosion resulting in change in formation temperature which in turn affects the rate of gas generation. Gas accumulation is considered to be dynamically controlled by gas generation from the source rock and gas loss at the updip section along a semi-permeable barrier (Gies, 1985). Gies also indicated from the particular pressure conditions in the tight gas reservoir that no downdip gas/water contact existed. In contrast, a hydrodynamic component responsible for the entrapment of the hydrocarbons in the Panhandle oil and gas field has been identified (Hubbert, 1940), suggesting the presence of a downdip gas-water contact and some hydraulic interconnection with the regional ground-water flow system. Therefore, the conditions described by Gies (1985) do not appear applicable in the Palo Duro Basin.

HYDROGEOLOGY

Geologic Setting

The Palo Duro Basin located in the central part of the Texas Panhandle is a cratonic basin that formed as a result of late Paleozoic tectonic activity. Major structural features such as the Bravo Dome, the Amarillo Uplift, and the Matador Arch shown in figure 4, represent the northern and southern boundaries of the Palo Duro Basin (Handford, 1980). The basin extends from the Tucumcari Basin in the west to the Hardeman Basin in the east.

8

DRAFT

The stratigraphy of the basin shows extreme hydrogeologic inhomogeneities caused by long-lived cycles of sedimentation in different environments (table 1). Handford and others (1980) distinguish four depositional cycles, reflecting the geologic development of the basin: (1) formation of the basin and subsequent deposition of basement-derived fan-delta granite wash from uplifts flanking the basin, (2) planation and burial of the uplifts through Early Permian time and infilling of the deep basin with shelf margin carbonate and basinal facies, (3) encroachment of continental red-bed facies from sources in New Mexico and Oklahoma and deposition of thick Middle to Upper Permian marine evaporites in arid environments, and (4) marine retreat during late Permian time and development of a Triassic lacustrine basin brought about as a result of continental rifting and drainage reversal. For detailed information on the tectonostratigraphic setting and depositional environment of the Palo Duro Basin refer to Handford and Dutton (1980) and Dutton and others (1982).

The most recent major tectonic events during Cenozoic time caused uplift and tilting of the basin. McGookey (1984) reported that the basin was uplifted by about 730 m (2,400 ft) in the southeast and by about 1,220 m (4,000 ft) in the northwest, probably largely during the last 10 to 15 million years. Prior to the uplift, the Palo Duro Basin was at or below sea level in Cretaceous time about 70 million years ago (McGookey, 1984).

Uplift of the basin created significant topographic relief and, most significantly, affected the hydrodynamics of the basin. Prior to the beginning of uplift in Miocene time (15 m.a.), it is assumed that only minor hydraulic gradients existed across the basin. During Cretaceous time (70 m.y.) and Early Miocene time, no major geologic events occurred that would have significantly modified the geometry of the Palo Duro Basin. This investigation is concerned with the hydrodynamic development of the Palo Duro Basin starting in Miocene time.

Besides tectonic events, other mechanisms such as deposition and erosion modify topography and can significantly affect the ground-water flow patterrn. In the Palo Duro Basin, three major post-Oligocene geomorphologic events can be identified: (1) deposition of the

9

DRAFT

Ogallala Formation, (2) erosion of the Pecos River valley, and (3) westward retreat of the Eastern Caprock Escarpment (erosion of the Rolling Plains).

Deposition of the Ogallala Formation started in Middle Miocene time (about 12 m.a.) (Bergren and Van Couvering, 1974; Tedford, 1981). The youngest caliche deposits were dated at about 2 to 6 million years (Izeet and others, 1972, 1981), giving a minimum age for Ogallala deposition. Limited geologic data from the Pecos River valley indicate that erosion occurred during the last 3 to 5 million years since the end of the Ogallala deposition (Thomas, 1972). Regional rates of westward retreat of the Caprock Escarpment were determined from time periods that range from 7,900 to 3,000,000 years and vary from 11 to 18 cm/yr (4.3 to 7.1 inches/yr) (Gustavson and others, 1981).

The major hydrogeologic units (Bassett and Bentley, 1982) in the Palo Duro Basin are the Deep-Basin Brine aquifer of Wolfcampian and Pennsylvanian age and the shallow Ogallala and Dockum aquifers, separated by a thick aquitard of Middle and Upper Permian evaporites (table 1). The San Andres unit 4 carbonate within the evaporite section can be considered an individual hydrologic unit. Dutton and Orr (in preparation) identified a regional flow system in the San Andres Formation, based on pressure and hydrochemical data.

Physiography and Climate

The main topographic features in the Texas Panhandle are the High Plains to the west and the Rolling Plains to the east. The surface of the High Plains is generally smooth and slopes gently eastward at about 2 to 3 m per kilometer (10 to 15 ft per mile) with an elevation decreasing from 1,500 to 975 m (4,920 to 3,200 ft) along the cross section (fig. 4). A gentle scarp forms its western limit in eastern New Mexico and the eastern limit is the Caprock Escarpment which has up to 300 m (1,000 ft) of relief. West of the Pecos River, the topography rises toward the Manzano mountain range, reaching an elevation of about 2,130 m (7,000 ft). The Rolling Plains to the east of the Caprock Escarpment are gently eastward dipping plains of low relief developed on relatively nonresistant rocks of Permian age.

10

DRAFT

The climate of the High Plains region is semiarid. The mean annual precipitation ranges from about 30 cm (12 inches) in the west to 58 cm (23 inches) in the east (Knowles and others, 1982). West of the Pecos River, precipitation generally increases toward the Manzano mountain range up to 50 cm (20 inches). The mean annual temperature of the High Plains is about $15°C$ (59°F) with an average difference between summer and winter temperatures of approximately $22°C$ (40°F).

Recharge and Discharge

Recharge to the Ogallala aquifer is estimated to range from 0.145 cm (0.058 inch) to 2.08 cm (0.833 inch) per year, depending on climate, vegetative cover, soil type, and clay or caliche aquicludes at the surface (Knowles and others, 1982). Along the cross section (fig. 4), recharge values assigned to the High Plains of the Texas Panhandle are at a minimum of 0.145 cm (0.058 inch) (Knowles and others, 1982), while in the New Mexico area, recharge rates to the High Plains may be higher due to a sandier soil type. The Pecos River is a major discharge area, primarily for ground water recharging to the west of the river (Mower and others, 1964). The San Andres Formation is the principal aquifer in this area and is recharged along the karstic outcrops west of the Pecos River (Gross and others, 1982). Discharge of ground water from the High Plains (Ogallala and Dockum aquifers) to the Pecos is probably small because of the eastward dipping strata and topography. Most of the ground water in the High Plains aquifer is discharged artificially through wells and naturally through springs and seeps along the Caprock Escarpment. Springs in the Rolling Plains east of the High Plains are characterized by high salinities due to salt dissolution by shallow ground water of Permian evaporite strata east of the Caprock Escarpment (Kreitler and Bassett, 1983; Richter, 1983). Discharge from the Deep-Basin Brine aquifer in the Palo Duro Basin probably occurs at the outcrop areas along the Wichita Uplift in Oklahoma.

11

DRAFT

DATA BASE

Hydraulic Head and Pressure

Abundant hydraulic head data from the Ogallala aquifer indicate that the shallow ground water generally moves east and southeast under the influence of the regional topographic dip (fig. 6). Although water levels have been declining since 1940, ground-water movement in the High Plains is only locally affected by pumpage creating a cone of depression where the water table is drawn down in the vicinity of the well (Knowles and others, 1982).

Hydraulic head data of the Deep-Basin Brine aquifer were derived from results of drill-stem tests and a limited number of pumping tests, which were converted into fresh-water heads. Wirojanagud and others (1984) evaluated pressure data and constructed a hydraulic head map for the Deep-Basin Brine aquifer (fig. 7). A comparison of hydraulic heads in the unconfined and confined aquifers (fig. 8) shows that heads in the Deep-Basin Brine aquifer are lower than heads in the Ogallala aquifer by up to 550 m (1,805 ft). Along the cross-sectional traverse, the hydraulic head difference beneath the High Plains is about 350 m (1,150 ft). The head difference generally decreases toward the south and to the east of the Caprock Escarpment where land surface drops abruptly by about 300 m (1,000 ft).

Dutton and Orr (1985) investigated the ground-water flow system of the San Andres Formation in eastern New Mexico and West Texas. In the Palo Duro Basin, the San Andres unit 4 carbonate within the Evaporite aquitard is considered regionally extensive and part of the overall San Andres aquifer system, indicating regional ground-water flow toward the southeast.

Hydrogeologic Properties

Estimation of realistic permeability of the different hydrogeologic units is important for the understanding of the hydrologic system of the Palo Duro Basin. In the following, the available information on the hydrologic characteristics of the different units are summarized.

12

DRAFT

Ogallala Formation

The Ogallala Formation consists primarily of fluvial clastics which were deposited over an irregular Triassic surface in a deltaic system of overlapping fan lobes (Seni, 1980). The percentage of sand and gravel generally decreases from west to east across the High Plains. Average hydraulic conductivity (arithmetic mean) of the Ogallala is 8.0 m/day (26.3 ft/day) based on pumping test results reported in Myers (1969). Vertical permeability was assumed to be one order of magnitude less than horizontal permeability, due to horizontal stratification of sands and muds in the formation.

Dockum Group

The Dockum Group represents a fluvial and lacustrine depositional system containing regionally extensive lacustrine mudstones. Percentage of sand within the Dockum varies between 40 percent and 10 percent (McGowen and others, 1979). Average hydraulic conductivity (arithmetic mean) for the Dockum sands is about 0.8 m/day (2.6 ft/day) based on pumping test results (Myers, 1969).

Most modeling approaches (INTERA, 1983; Wirojanagud and others, 1985) assume that the potentiometric surface of the Ogallala is representative of the Dockum as well. There is evidence, however, that hydraulic heads in the Dockum are significantly lower (30 to 90 m, 100 to 300 ft) than those in the Ogallala (Fink, 1963; Dutton and Simpkins, 1985). Also, the water chemistry and the O^{18} and H^2 concentration of ground water in the Dockum is different from that in the overlying Ogallala aquifer (Dutton and Simpkins, 1985), suggesting that the two aquifers are not well interconnected.

Because of the regionally extensive lacustrine mudstones, vertical permeability of the Dockum is probably very low. As shown in Simulation D of this study, vertical permeability has to be at least four orders of magnitude lower than horizontal permeability in order for the model to simulate a significant head difference of up to 30 m (100 ft) between the Ogallala and Dockum aquifers.

13

DRAFT

Permian Evaporite Strata

The Permian evaporite strata include deposits of evaporites, and of inner shelf systems (fig. 4). The Evaporite aquitard in the Palo Duro Basin consists mainly of thick layers of salt deposits, anhydrite, red beds, and peritidal dolomite (McGowen, 1981). A vertical permeability of 0.00028 md for the Evaporite aquitard was estimated by taking the harmonic mean of permeabilities representing each substrata (Wirojanagud and others, 1984). Permeabilities for the substrata are based on field measurements and typical values for the geologic material. This permeability value is at best a rough estimate and does not incorporate possible effects of fractures which could increase locally vertical leakage through the evaporite section.

San Andres Unit 4 Carbonate

The San Andres Formation in the Palo Duro Basin consists primarily of low permeable salt, anhydrite, carbonate, and mudstone. The San Andres unit 4 carbonate is regionally extensive in the Palo Duro Basin (fig. 5), with a thickness ranging from 15 to 25 m (50 to 80 ft). Permeabilities in the San Andres unit 4 carbonate range from 0.1 md to 0.5 md, based on data from drill stem and pumping tests from six DOE test wells. Toward the Midland Basin to the south, a facies change in the San Andres Formation from generally evaporite strata to marine strata results in a significant increase in permeability (Dutton and Orr, 1985).

Lower Permian and Pennsylvanian Strata

Lower Permian, Pennsylvanian, and Pre-Pennsylvanian formations constitute the Deep-Basin Brine aquifer (table 1). The depositional environments were similar during Lower Permian (Wolfcampian) and the Pennsylvanian and consisted of (fig. 4) (1) fan-delta system, (2) shelf and shelf-margin systems, and (3) a basinal system (Handford and Dutton, 1980; Dutton and others, 1982). The fan-delta system is composed of arkosic sands and conglomerates (granite wash) which were derived from the igneous and metamorphic uplifts surrounding the Palo Duro Basin. Open marine shelf carbonates and terrigenous muds comprise the shelf and basinal system. The top of the Wolfcamp is marked by a basinwide distribution of shelf-margin facies (brown

14

DRAFT

dolomite) that resulted from a southward shift of the shelf break, which terminated deposition of basinal facies in the area (Handford, 1980).

Wirojanagud and others (1984) combined permeability data based on limited analyses of drill stem tests, pumping tests, and compiled data by Core Laboratories, Inc. (1972) and derived average permeabilities and variances of the different hydrologic units within the Deep-Basin Brine aquifer (table 2). The calculated geometric mean of permeabilities for Wolfcampian and Pennsylvanian carbonates is 8.9 and 17.9 md, respectively. Granite wash and pre-Pennsylvanian strata yielded permeabilities of 8.6 md and 4.76 md, respectively. For comparison, average permeability values and variances for the different types of tests were compiled by Smith (1983). The geometric mean rather than the arithmetic mean was used to account for the fact that the substrata within which permeability was measured tend to be discontinuous. Theoretically, if the strata are horizontally continuous, the arithmetic mean is appropriate, but if the strata are randomly discontinuous, a geometric mean may be more appropriate (Warren and Price, 1961).

Vertical permeability for the Lower Permian and Pennsylvanian strata is assumed to be two orders of magnitude lower than horizontal permeability due to the horizontal stratification within each hydrologic unit. Values of permeability were converted to hydraulic conductivity using an average fluid salinity and temperature of 127,000 mg/L and 46°C (115°F), based on data from Bassett and Bentley (1982). For these fluid properties 1 md equals 0.00115 m/day.

The permeability data from the Deep-Basin Brine aquifer show large variances (natural log) of up to 7.13, indicating an extremely heterogeneous distribution of permeabilities and a relatively small data base (table 2). Proximal granite-wash deposits closer to the source areas (Amarillo Uplift, Bravo Dome, and Wichita Mountains) apparently have higher permeabilities than distal granite-wash deposits in the center of the basin. Five pumping tests from proximal granite wash in the J. Friemel #1 well located in northeastern Deaf Smith County yielded permeabilities of 40 md to 250 md with an average of 140 md, which is much higher than the

15

DRAFT

geometric mean of 8.6 md. Relatively high permeabilities of 250 md in proximal granite wash were also suggested by Wirojanagud and others (1984).

Data on measured permeability for the mud-flat and alluvial fan-delta systems of Permian to Pennsylvanian age (fig. 5) below the Pecos Plains were not available. Therefore, a generic value of permeability of about 70 md (equivalent to a hydraulic conductivity of 8.2×10^{-2} m/day) as suggested by Bassett and others (1981) was assigned to the westernmost hydrologic unit based on typical values for comparable geologic materials (Freeze and Cherry, 1979). Using this typical permeability value, the model computed a discharge rate to the Pecos River of about 1.3 m^3/day, which is in reasonable agreement with reported data on rate of streamflow increase along the Pecos River in this area (Mower and others, 1964).

Salt Dissolution Zones

Permeabilities for the units representing the salt dissolution zones located east and west of the High Plains in figure 5 were conservatively estimated to be 70 md (equivalent to 0.082 m/day). This value is much higher than the permeability of the adjacent aquitard (fig. 5) due to intense faulting and collapse of the formation overlying the salt deposits. Recent hydrologic testing in the DOE salt dissolution wells yielded relatively high hydraulic conductivities of about 0.17 m/day (Dutton, 1985). The eastward extension of the Permian salt strata is represented by a mudflat system (fig. 5) with permeabilities derived from generic values as suggested by Bassett and others (1981).

Specific Storage

Investigating transient ground-water flow conditions requires information on the specific storage of the different hydrologic units. In-situ measurements of storativity in deep formations are difficult to obtain and therefore generally unavailable. Values of specific storage used in the model are based on data obtained for geologic materials as reported by Domenico and Miflin (1965). Their data on specific storage were used by several investigations

16

DRAFT

dealing with non-steady flow of fluids in sedimentary basins (Bredehoeft and Hanshaw, 1968; Tóth and Millar, 1983). In the present model, the value of specific storage for all the different hydrologic units is assumed to be 0.0001 m^{-1}. This value is comparable to values used by Tóth and Millar (1983) for the deeper units in the Alberta Basin. For the shallow Ogallala aquifer, the assigned value is no doubt too low because of the water-table conditions. However, the discrepancy has a negligible effect on transient response of the Deep-Basin Brine aquifer because the shallow aquifers constitute a small fraction of the total thickness represented in the model. Dissipation of pore pressures are represented by the hydraulic diffusivity which is defined as

$$D = \frac{K}{S_s}$$

where K is the hydraulic conductivity and S_s is the specific storage. A decrease in hydraulic diffusivity will cause hydraulic heads to equilibrate slower to changes of the boundary value.

COMPUTER PROGRAM

The model was implemented with the computer programs FREESURF, developed by Neuman and Witherspoon (1970) and FLUMPS (Neuman and others, 1982). FREESURF was used to solve the partial differential equation describing two-dimensional steady-state ground-water flow in porous media:

$$\frac{\partial}{\partial x} \left(K_x \frac{\partial h}{\partial x} \right) + \frac{\partial}{\partial z} \left(K_z \frac{\partial h}{\partial z} \right) = 0$$

where K_x and K_z are horizontal and vertical hydraulic conductivity, respectively, and h is hydraulic head. FREESURF uses a finite element method and a direct solution technique (Gaussian elimination).

The program computes hydraulic heads at each node and fluxes along prescribed head boundaries representing recharge or discharge. In addition, the program was used to compute the stream functions at each node based on the results of the steady-state hydraulic heads and

17

DRAFT

fluxes along the inflow and outflow boundaries. For details concerning the computation of streamlines, refer to Fogg and Senger (1985).

Transient ground-water flow simulations were performed using the computer program FLUMPS. FLUMPS is a modification from the original version of the program FLUMP developed by Narasimhan and others (1977, 1978). FLUMPS was used to solve the partial differential equation describing two-dimensional transient ground-water flow in porous media:

$$\frac{\partial}{\partial x}\left(K_x \frac{\partial h}{\partial x}\right) + \frac{\partial}{\partial z}\left(K_z \frac{\partial h}{\partial z}\right) = S_s \frac{\partial h}{\partial t}$$

where K_x and K_z are horizontal and vertical hydraulic conductivities, respectively, and S_s is the specific storage. FLUMPS employs the finite element method for solving linear and nonlinear ground-water flow problems in two-dimensional and quasi three-dimensional configurations using either a direct solution technique or an iterative solution technique. The program computes hydraulic heads at each node, fluxes between adjacent nodes, and fluxes along prescribed hydraulic-head boundaries representing recharge and discharge. In addition, the model allows hydraulic heads to vary with time, and hydraulic properties to vary with time or hydraulic head.

MODELING PROCEDURE

Finite Element Mesh

The ground-water flow model was constructed along an east-west cross section extending from New Mexico across the Texas Panhandle into Oklahoma (fig. 5). The finite element mesh was designed to represent the geometry of the different depositional facies (fig. 9). Due to extreme vertical exaggeration, the large node spacing differences between horizontal and vertical directions could cause theoretically numerical errors in the solution. As demonstrated in Appendix A, however, these errors are negligibly small in the models of this study.

18

In figure 9, three hydrologic units are distinguished within the Deep-Basin Brine aquifer, based on the lithostratigraphy: (1) carbonate shelf and shelf-margin systems, (2) mud-filled basin and slope system, and (3) fan delta system (granite wash). The Permian evaporite sequence is represented as a thick aquitard separating the Deep-Basin Brine aquifer from the overlying Ogallala and Dockum fresh-water aquifers. Within the Evaporite aquitard, the San Andres unit 4 carbonate is distinguished as an individual hydrologic unit which separates the evaporite sequence into a lower and upper aquitard.

Additional hydrogeologic units represented in the model (fig. 9) are the salt dissolution zones to the east and to the west of the High Plains, the Permian mudflat system extending into Oklahoma, and the Permian/Pennsylvanian mudflat and alluvial fan delta systems in New Mexico.

Boundary Conditions

In the steady-state ground-water flow model implemented with the computer program FREESURF, two types of boundary conditions are applied: (1) prescribed heads (Dirichlet boundary condition) and (2) prescribed flux (Neumann boundary condition). The upper surface of the finite element mesh corresponds approximately to the water table and generally follows the topography (water-level declines caused by ground-water pumpage are ignored in the model). To the east and west of the High Plains, the water table is represented with prescribed head boundary conditions. Information on the amount of recharge to the Ogallala aquifer along the High Plains (Knowles and others, 1982) permitted assignment of prescribed fluxes at the corresponding boundary nodes. A recharge value of 0.145 cm/yr (0.058 inch/yr) was assigned along the High Plains in the Texas Panhandle and increased to 0.625 cm/yr (0.250 inch/yr) to account for the sandier soil type in the New Mexico area of the High Plains.

The lower boundary of the mesh was assumed to be impervious and corresponds to the contact between the Deep-Basin Brine aquifer and basement rocks. Hydraulic head was assumed to be uniform with depth implying horizontal flow on the eastern boundary. This is

19

DRAFT

consistent with pressure-depth data from Jackson County, Oklahoma (located approximately at the eastern edge of the cross section), which show a slope of the pressure-depth regression line equivalent to brine-hydrostatic (fig. 10).

Boundary conditions in the transient model are the same as in the steady-state model, except that prescribed heads are used along the entire upper surface of the mesh. Modification of topography as a result of tectonic and geomorphologic activity is simulated in the model by varying prescribed heads with time along the upper surface of the mesh. Prescribed heads along the eastern boundary of the mesh were set equal to the water table at the surface node and heads were assumed to be uniform with depth throughout the simulations. Similarly, hydrocarbon production which causes a decline in reservoir pressures was simulated by reducing hydraulic heads with time at the particular node location in the model representing a hydrocarbon reservoir.

LIMITATIONS OF THE MODEL

When comparing the results of the model with observed data, it is important to recognize that the regional ground-water flow direction in the deep aquifer (fig. 7) ranges from eastward to northeastward and ground-water flow in the Ogallala aquifer (fig. 6), as well as in the San Andres Formation (Dutton and Orr, 1985), is toward the southeast. The cross-sectional model depicts ground-water flow from west to east. Thus, results of the model are not always directly comparable to field conditions. For example, hydraulic conductivities had to be reduced by one order of magnitude in both the Ogallala and Dockum aquifers in the western High Plains in New Mexico using the reported recharge rates in order for the model to produce the observed water levels of the Ogallala aquifer with reasonable accuracy. This artificial reduction in hydraulic conductivity does not necessarily represent a calibration of "true" aquifer properties based on the available hydraulic head data but may reflect the discrepancy in vertical geometry between

20

DRAFT

the actual northwest to southeast flow direction of the High Plains aquifer and the imposed west-east flow direction in the cross-sectional model.

Despite the errors associated with modeling of the basin in two dimensions rather than three, the model includes the major hydrogeologic components that tend to dominate the flow system: (1) topographic relief and, in particular, the tilted surface of the High Plains, and (2) the overall hydrostratigraphy, including the low permeability aquitard and the relatively permeable granite-wash deposits. Thus, the model provides a valid approximation of several aspects of the basin-scale hydrodynamics.

Discretization of the cross-sectional model required simplification and conceptualization of the lithostratigraphy of the basin. Ground-water flow pattern on a local scale could therefore be much more complex than those depicted by the model.

Major potential sources of errors in the model are the estimates of hydraulic conductivities and assumed anisotropies of the different hydrologic units. With the exception of the granite wash, which was subdivided into distal and proximal deposits, uniform permeabilities were assigned to the hydrologic units in the deep section ignoring possible lateral and vertical permeability trends throughout the basin. Large values of variance of measured permeabilities (table 2) suggest large natural variations in permeabilities of the hydrologic units. The data are, however, insufficient to map spatial permeability distributions within the different units. For some units where measured permeability values were not available (i.e., Evaporite aquitard, Permian/Pennsylvanian mudflat and alluvial/fan delta system), assumed permeability values had to be used based on typical values for the geologic material.

Another limitation of the model is the assumption that fluid is homogeneous throughout the basin; that is, density and temperature effects were omitted in the model. Because of increased salinities at depth, the increase in fluid density leads to greater gravitational forces, and to an increase in viscosity. Increased viscosity results in a decrease of hydraulic conductivity and decreases flow rates in a linear fashion. The errors, however, are thought to be small compared to errors in permeability values.

21

DRAFT

Simulating transient flow conditions requires information on specific storage of the hydrogeologic units. Specific storage of a saturated aquifer represents the volume of water than can be removed from or taken into storage as a result of a change in hydraulic head. Therefore, specific storage in addition to hydraulic conductivity is important with regard to propagation of transient conditions through the aquifer. Pumping tests performed in DOE wells in the Deep-Basin Brine aquifer were not designed to yield data of storativity. The assigned values of specific storage are based on typical and measured values reported in the literature (Domenico and Mifflin, 1965; Freeze and Cherry, 1979) that range from 0.005 to 0.00005 m^{-1}. The value of specific storage of 0.0001 m^{-1} used in the model is the same as the value used by Tóth and Millar (1983) for the deeper units in the Red Earth region of the Alberta Basin.

Simulation of uplift, deposition and erosion was performed in a simplistic way. Without changing geometry of the finite element mesh, prescribed head boundary conditions along the upper surface and along the eastern boundary of the mesh were varied so as to represent the change in water table as a result of the modification of topography. In other words, even though the pre-erosion scenario included shallow aquifer volume, this is not accounted for in the model (fig. 9) when simulating pre-erosion conditions. Thus, in the pre-erosion simulations, transmissivity of certain parts of the represented shallow aquifers is somewhat low and leakance (vertical hydraulic conductivity divided by thickness) is somewhat high. The magnitude of these errors is presumably small compared to other errors in the permeability data. Furthermore, these errors primarily affect the shallow system and do not seriously affect the rate of propagation of surface boundary effects into the deeper units.

Detailed information on the timing and the extent of the different tectonic and geomorphologic events is scarce. The general sequence and timing of the different tectonic and geomorphologic processes were modeled in successive simulations, ignoring possible overlapping of events. This approach nevertheless allowed us to test the effects of individual tectonic and geomorphic events on the general ground-water flow regime.

22

DRAFT

SIMULATION STRATEGY: STEADY-STATE MODEL

Different simulations were run to investigate the effect of hydrostratigraphy and topography on ground-water flow in the Palo Duro Basin (table 3). The purpose of the simulations was not necessarily aimed at achieving the best fit with the observed head data. The primary objective was to investigate the importance of various factors affecting the overall ground-water flow pattern in the basin.

Simulations A-1 and A-2 test possible spatial permeability variations of granite-wash deposits. While in Simulation A-1 a uniform permeability distribution for granite wash (k = 8.6 md) is used throughout the basin (table 2), in Simulation A-2 proximal granite wash deposits in the eastern part of the cross section are assigned a permeability value of 100 md, which is in the range of the average value of measured permeabilities for granite wash in DOE J. Friemel #1 well. Simulation A-3 incorporates the possible effect of proximal granite-wash deposits along the Oldham Nose and the Amarillo Uplift north of the cross-sectional traverse by inserting artificially high values of granite-wash permeability throughout the entire east-west cross section. Although computed heads in Simulation A-3 agree better with kriged heads in the deep section, Simulation A-2 is considered the most realistic model supported by the permeability data which are presently available for the Deep-Basin Brine aquifer.

Simulations B-1 to B-3 investigate the effect of leakage through the Evaporite aquitard by only varying vertical permeability of the aquitard. Permeability of the aquitard is increased one order of magnitude to 2.8×10^{-3} md in Simulation B-1 and decreased one and two orders of magnitude in Simulations B-2 and B-3 to 2.8×10^{-5} md to 2.8×10^{-6} md, respectively. Also, the effect of the San Andres unit 4 carbonate on leakage through the Evaporite aquitard was investigated in Simulations B-1 to B-3.

The hydraulic interconnection between the Ogallala and the Dockum was addressed in Simulation C. By reducing vertical permeability of the Dockum in successive runs, the observed

23

DRAFT

hydraulic head differential in the shallow aquifer system was modeled and its effect on leakage rate through the Evaporite aquitard, and on heads in the deep section, is investigated.

In previous work, Senger and Fogg (1983) showed that the Pecos River does not represent a complete ground-water flow divide for the deep aquifer section but allows limited underflow of ground water. However, the ground-water flow regime is strongly affected by the Pecos River, which captures most of the ground water recharging in the New Mexico area west of the Pecos River and reduces potential recharge to the Deep-Basin Brine aquifer in the center of the basin. In Simulation D, the effect of the Pecos River on the subhydrostatic conditions in the Deep-Basin Brine aquifer is tested. For this purpose, the finite element mesh is modified to eliminate the topography of the Pecos River valley by extending the general slope of the High Plains surface toward the mountain range at the western boundary of the cross section (fig. 19).

RESULTS AND DISCUSSION

Granite-Wash Permeability

Simulation A-1

In Simulation A-1, hydraulic conductivities of the different hydrologic units were assigned according to table 4. The permeability value for the shelf carbonate in the Deep-Basin Brine aquifer is a thickness-weighted arithmetic average of permeabilities (geometric means) of the Wolfcampian carbonate, Pennsylvanian carbonate, and pre-Pennsylvanian rocks.

Hydraulic heads computed by the model in Simulation A-1 indicate two different flow regimes (fig. 11): (1) a shallow flow system governed primarily by topography, and (2) a deeper flow regime recharging in the New Mexico area and passing deep beneath the Pecos River, which acts as a ground-water flow divide in the upper part of the cross section. The thick evaporite section in the center of the cross section segregates the two flow systems.

Most importantly, Simulation A-1 produced most of the underpressuring observed beneath the High Plains yielding hydraulic heads in the Deep-Basin Brine aquifer (beneath the High

24

DRAFT

Plains) that are up to 250 m (820 ft) lower than hydraulic heads in the Ogallala (fig. 11). The observed head difference between the Ogallala aquifer and Deep-Basin Brine aquifer (fig. 7) is about 350 m (1,150 ft) in the area of the High Plains. These results suggest that most of the underpressuring is due to a topographic effect, which corresponds to "apparent underpressuring" according to the definition given by Orr and Kreitler (1985). The water table of the Ogallala aquifer on the High Plains is elevated above the recharge and discharge areas of the Deep-Basin Brine aquifer that flank the High Plains to the east and west. In addition, the Ogallala and Dockum aquifers are effectively isolated from the Deep-Basin Brine aquifer, maintaining a steep head differential. The shallow water-table system is somewhat analogous to a perched aquifer.

East of the Caprock Escarpment, the model computed unrealistic hydraulic heads in the deep section that become progressively higher by up to 93 m (305 ft) than hydraulic heads in the shallow unconfined section (fig. 11). In contrast, figure 8 shows that hydraulic heads east of the Caprock Escarpment do not exceed land surface elevation. Only toward the Texas-Oklahoma border do kriged heads in the deep section approach hydrostatic conditions. Simulation A-2 shows that this discrepancy is caused by the permeability distribution in the granite wash.

Simulation A-2

As mentioned earlier, higher permeability values are more likely in proximal granite-wash deposits in the eastern part of the cross section than in distal granite wash in the center of the basin owing to a presumed decrease in grain size away from the source area. In Simulation A-2, a permeability value of 100 md was assigned to granite wash east of the Caprock Escarpment in the proximal facies. As a result, computed hydraulic heads in the Deep-Basin Brine aquifer east of the escarpment no longer exceed heads in the shallow interval (fig. 12). Moreover, the simulated hydraulic head differential between the Ogallala and the Deep-Basin Brine aquifer increased from 250 m (820 ft) to 350 m (1,150 ft).

25

DRAF

In general, the computed heads in the eastern half of the cross section show good agreement with kriged head data in the Deep-Basin Brine aquifer. These results demonstrate the importance of the relatively permeable granite-wash deposits. The granite wash effectively drains the deeper section with greater ease than is recharged.

In the western half of the cross section computed heads in the deep section become progressively higher by up to 300 m (1,000 ft) than kriged heads in both Simulations A-1 and A-2. Because of the distance of about 150 km (93 miles) from the Texas-New Mexico border to the Caprock Escarpment in the east, the draining effect of the relatively permeable granite-wash deposits in the east does not influence the western part of the Deep-Basin Brine aquifer. The discrepancy in hydraulic heads could be an artifact of the geometry and the direction of the cross-sectional model. Wirojanagud and others (1985) show that relatively permeable granite-wash deposits along the Amarillo Uplift and Bravo Dome are important factors controlling the regional ground-water flow direction in the Deep-Basin Brine aquifer. Proximal granite wash occurring to the north of the cross section (fig. 13) was found to have good permeability as indicated by pumping test results in the J. Friemel #1 well located in northeastern Deaf Smith County. The possible draining effect of these deposits, however, is not considered in the east-west cross-sectional model which could explain the discrepancy between computed hydraulic heads and the kriged heads in the western part of the Deep-Basin Brine aquifer.

Figure 12 also shows the computed streamlines which correspond to the head solution in Simulation A-2. The region defined by two adjacent streamlines contains a constant volumetric flow rate. The streamline distribution shows that ground-water flow is concentrated in the shallow aquifer system. Each streamtube in the shallow section (shaded pattern) carries 0.2 m^3/d while each streamtube in the deeper section carries only 0.01 m^3/d. Only 0.033 m^3/d, or less than 0.1 percent of the total ground-water inflow of 4.47 m^3/d, recharges to the Deep-Basin Brine aquifer from the west and 0.0125 m^3/d recharges via vertical leakage across the Evaporite aquitard beneath the High Plains into the deep aquifer.

26

DRAF

The streamline distribution in figure 12 shows that ground water within the Deep-Basin Brine aquifer is flowing down the structural dip into the central basin. East of the central basin ground-water flow is focused into the more permeable granite-wash deposits and discharge occurs laterally through the eastern boundary.

Simulation A-3

The purpose of this simulation is to consider possible draining effects of proximal granite wash to the northeast of the cross section along the Amarillo Uplift and Oldham Nose, by inserting artificially high values of granite-wash permeability along the entire east-west cross section. In addition, information on the occurrence of thick granite-wash deposits in northeastern New Mexico (Siminitz, 1985) was incorporated in the model by extending the Permian-Pennsylvanian fan-delta system into New Mexico. Granite-wash permeability was increased from 8.6 md to 100 md for distal facies to the west and from 100 md to 250 md for proximal granite wash to the east of the Caprock Escarpment. As mentioned earlier, pumping-test results in J. Friemel #1 well indicated permeability values of up to 400 md for proximal granite wash.

The computed hydraulic heads (fig. 14) in the Deep-Basin Brine aquifer are significantly lower in the western part of the cross section compared to the previous Simulation A-2. Overall, heads in the deep section agree reasonably well with kriged heads in figure 6. The corresponding streamlines in figure 14 show that the amount of ground-water inflow from the west into the Deep-Basin Brine aquifer increased from 0.033 in Simulation A-2 to 0.074 m^3/day and flow follows predominantly the permeable granite wash deposits. Leakage through the Evaporite aquitard under the High Plains increased from 0.0125 in Simulation A-2 to 0.0155 m^3/day in this simulation due to the increased hydraulic gradient across the Evaporite aquitard predominantly in the western part. Increased permeabilities of the porous shelf margin carbonates in the Permian and Pennsylvanian strata (Handford and Dutton, 1980; Conti and others, 1984) were considered to be important in the horizontal-plane ground-water flow model

27

DRAFT

in Wirojanagud and others (1984). In another simulation of this model, increased permeabilities along the shelf margins did not significantly change hydraulic heads and the overall ground-water flow pattern in the deep section in the cross-sectional model. The resulting decrease of hydraulic heads in the western part of the Deep-Basin Brine aquifer in Simulation A-3 compared to Simulation A-2 further indicates the importance of the granite-wash deposits acting as a hydrologic sink.

Role of the Evaporite Aquitard on Subhydrostatic Conditions

The Evaporite aquitard is thought to be an important cause of the subhydrostatic conditions in the deep aquifer because it isolates the deep basin system from the higher hydraulic heads in the Ogallala and Dockum aquifers. In other words, if the Evaporite aquitard were absent, the Deep-Basin Brine aquifer and the Ogallala and Dockum aquifers would be hydraulically connected and their heads would be similar. In the following simulations, the role of the aquitard is tested by first increasing and then decreasing aquitard permeability. Also, by investigating the effects of varying aquitard permeabilities on the head distribution in the deep section, a range of possible aquitard permeabilities is estimated.

In this context, the effect of the San Andres unit 4 carbonate on leakage through the Evaporite aquitard is evaluated. Because of the higher permeability and regional extent throughout the Palo Duro Basin, the San Andres unit 4 carbonate could capture some of the downward leakage and discharge it laterally along the outcrop east of the Caprock Escarpment. Varying aquitard permeabilities will help determine whether ground-water flow in the San Andres unit 4 carbonate is primarily vertical or horizontal on a regional scale.

Simulation B-1

Increasing aquitard permeability from 2.8 x 10^{-4} md (Simulation A-2) to 2.8 x 10^{-3} md in Simulation B-1 results in a significant increase in hydraulic heads of up to 250 m in the deep section (fig. 15). The computed streamlines in figure 15 show that considerably more ground

28

DRAFT

water is recharged to the deep section via vertical leakage across the Evaporite aquitard (0.059 m^3/d) than through lateral flow from the west (0.014m^3/d). The computed heads became unrealistically high which suggests that the generically-derived permeability value of 2.8 x 10^{-4} md (Simulation A) represents an upper limit of possible permeability values for the Evaporite aquitard. In comparison, Wirojanagud and others (1984) inferred a permeability value of 8 x 10^{-5} md from their "best" simulation of a horizontal-plane ground-water flow model.

Simulation B-2

The permeability value assigned to the Evaporite aquitard was decreased from 2.8 x 10^{-4} md in Simulation A-2 to 2.8 x 10^{-5} md in this simulation. The distribution of hydraulic heads and streamlines (fig. 16) indicates an increase in lateral flow within the San Andres Cycle 4 dolomite, and somewhat reduced hydraulic heads in the deep basin aquifers by up to 37 m (121 ft) compared to Simulation A-2. Vertical leakage through the Evaporite aquitard beneath the High Plains decreased from 0.0125 m^3/d in Simulation A-2 to 0.0015 m^3/d in this simulation.

Simulation B-3

Aquitard permeability was decreased by 2 orders of magnitude from 2.8 x 10^{-4} md (Simulation A-2) to a very low permeability value of 2.8 x 10^{-6} md which represents the lowest range of typical aquitard permeabilities listed in Freeze and Cherry (1979). The results in figure 17 show a general decrease of hydraulic heads in the Deep-Basin Brine aquifer by up to 41 m (135 ft) in the central part of the cross section compared to Simulation A-2. In the western part of the deep section, changes in computed heads were much smaller, indicating that a drastic decrease of leakage through the Evaporite aquitard (approximately 10^{-4} m^3/day) does not significantly reduce computed hydraulic heads in eastern New Mexico.

The computed streamlines show that ground water recharging west of the Pecos River flows beneath the Pecos River into the San Andres unit 4 carbonate (fig. 17). Approximately at the center of the cross section, all of the ground water recharged from the west leaked

29

downward into the deeper units. Thus, in the eastern half of the cross section, the model indicates that all of the ground water in the San Andres Formation originates as leakage from the overlying hydrologic units.

The topographic effect of the Pecos River valley to restrict underflow of San Andres water recharging from the west is probably not as significant as depicted by the model. The regional ground-water flow pattern in the San Andres Formation (fig. 8) is northwest to southeast and ground-water flow in northeastern New Mexico is approximately parallel to the course of the Pecos River. Thus, capture of recharge water in the San Andres Formation along the Pecos River occurs primarily further to the south toward the Midland Basin (fig. 8) where flow is more perpendicular to the Pecos River and therefore suggests greater discharge to the river.

The previous simulations (B-1 to B-3) suggest that: (1) the generically derived permeability value ($k = 2.8 \times 10^{-4}$ md) for the Evaporite aquitard represents the upper limit of possible aquitard permeability. (2) To achieve predominantly lateral ground-water flow within the San Andres unit 4 carbonate the permeability ratio between San Andres unit 4 carbonate and the Evaporite aquitard has to be greater than 10^5, in order to trace a horizontal streamline halfway across the basin. In another simulation with aquitard permeability reduced to 2.8×10^{-7} md, the model indicated a horizontal streamline through the entire San Andres unit 4 carbonate from the recharge area in New Mexico to the discharge zone east of the Caprock Escarpment.

Toward the Midland Basin, the San Andres Formation facies changes from an evaporitic unit consisting primarily of salt, anhydrite, and mudstone, into a normal marine carbonaceous unit resulting in significantly higher permeability of the San Andres Formation and a concomitant increase in the permeability contrast between aquifer and aquitard. In addition, the overall head gradient across the Evaporite aquitard decreases toward the Midland Basin. Lateral flow in the San Andres Formation is more likely in the Midland Basin area than in the Palo Duro Basin. In the latter, the aquitard permeability on a regional scale would have to be

30

DRAFT

unrealistically low (less than 10^{-6}-md) to produce complete lateral flow in the San Andres unit 4 carbonate across the basin. The San Andres unit 4 carbonate is characterized by permeabilities of less than 0.5 md based on a limited number of drill-stem tests (Dutton and Orr, 1985). Only the occurrence of open fractures within the San Andres unit 4 carbonate could significantly increase the effective permeability of this unit and allow lateral flow over long distances through the dolomite unit.

Interconnection of Ogallala and Dockum Aquifers

In the previous simulations, the Ogallala and Dockum aquifers were well-interconnected inasmuch as vertical flow between the two aquifers was not restricted by low values of hydraulic conductivity. Accordingly, heads did not differ appreciably between the two aquifers. However, Fink (1963) and Dutton and Simpkins (1985) indicate that in some areas hydraulic heads in the Santa Rosa member of the Dockum are about 30 to 100 m (100 to 300 ft) lower than heads in the Ogallala. To model a significant hydraulic head difference across the shallow aquifer system, vertical hydraulic conductivity of the Dockum was lowered in successive runs of the model until the minimum observed head difference was simulated in the model. A significant head difference between the Ogallala and the Dockum results in reduced hydraulic gradients across the evaporite section, which in turn reduces the amount of leakage through the Evaporite aquitard.

Simulation C

Using K_z = 8 x 10^{-2} m/day for the Ogallala and K_z = 8 x 10^{-5} m/day for the Dockum (2 and 4 orders of magnitude lower than K_x, respectively), computed heads in the Dockum were lower than in Simulation A-2 by up to 75 m (246 ft) in the western part of the High Plains (fig. 16). The difference in computed hydraulic heads between the Ogallala and the Dockum, however, generally decreases toward the east, and Dockum heads in the vicinity of the escarpment become slightly higher than Ogallala heads (fig. 18).

31

DRAFT

The change in vertical hydraulic gradient in the shallow aquifer system results in slightly lower heads in the deep section (less than 5 m or 16 ft) and an increase in Ogallala heads in the western part (up to 40 m or 131 ft) compared to Simulation A-2. The hydraulic head difference across the Evaporite aquitard decreases relative to that in Simulation A-2 reflecting the decrease in heads at the base of the Dockum due to reduced flow between the Ogallala and Dockum. The general ground-water flow pattern in the deep section as shown by the computed streamlines (fig. 18) does not change noticeably. However, leakage through the evaporites beneath the High Plains decreased from 0.0125 m^3/day to 0.0108 m^3/day, which is a 14 percent reduction in leakage rate from that in Simulation A-2. Thus, vertical hydraulic gradients in the shallow aquifer systems and their effect on leakage through the Evaporite aquitard could be important.

Keep in mind that, because of the two-dimensionality of the cross-sectional model, the lateral head distribution in the upper and lower aquifer was neglected. In reality, regional flow in the shallow aquifer is in a southeasterly direction, while flow in the deep aquifer is more toward the northeast. The different flow directions could affect the overall head difference between the two aquifer systems.

Effect of the Pecos River

In order to evaluate the effect of the Pecos River on subhydrostatic conditions in the Palo Duro Basin, the finite element mesh was modified in Simulation D such that hydraulic heads prescribed on the upper boundary extended in a straight line from the western caprock escarpment to the Manzano mountain range in New Mexico, thereby eliminating the Pecos River valley as a major discharge area. In this model, additional recharge to the High Plains aquifer occurs by ground water recharging west of the Pecos River and flowing into the Ogallala and Dockum aquifers, which results in relatively higher hydraulic heads in the High Plains aquifer as compared to the previous simulations.

32

DRAFT

Simulation D

Computed heads in figure 19 increase significantly in the western part of the Deep-Basin Brine aquifer relative to computed heads in Simulation A-2 (fig. 12). Heads in the eastern part, however, do not change appreciably (less than 30 m), and still display underpressured conditions. Ground-water flow into the Deep-Basin Brine aquifer, west of the Pecos River, increases from 0.033 m^3/day in Simulation A-2 to 0.054 m^3/day in this simulation (fig. 19). In the western half of the deep aquifer beneath the High Plains the computed streamlines indicate upward leakage of deep basinal fluids through the overlying Evaporite aquitard of about 0.0064 m^3/day. Underpressured conditions in the eastern part of the basin result in flow reversal with downward leakage across the Evaporite aquitard. In the New Mexico area, the streamline distribution indicates that most of the flow lines are still deflected upward to the surface at the facies contrast between the Permian-Pennsylvanian mudflat and fan-delta system to the west and the Evaporite aquitard in the center of the cross section. Hence, the facies contrast rather than topography is the more important cause of upward flow of ground water beneath the Pecos Valley. The increase in ground-water recharge to the deep section in Simulation D affects hydraulic heads in the western half of the cross section. However, heads in the eastern part did not change significantly, indicating that the topographic effect of the Pecos River on the hydrologic regime is restricted to the updip section of the Deep-Basin Brine aquifer. Ground-water discharge to the Pecos does not significantly affect subhydrostatic conditions in the eastern part of the cross section.

The effect of the Pecos River on hydraulic heads in the deep section would probably increase if the relatively permeable granite-wash deposits extended far into the New Mexico area, which could result in an increase of ground-water flow from the west into the Deep-Basin Brine aquifer. However, our geologic data indicate that granite-wash deposits are pinching out east of the Pecos (Handford and others, 1981). Furthermore, head maps from the Deep-Basin Brine aquifer (Smith and others, 1985; SWEC, 1983) show steep hydraulic gradients in eastern

33

DRAFT

New Mexico which suggest a zone of low permeability in the deep section. This would restrict possible underflow beneath the Pecos River of recharge water from the western outcrop area.

Ground-Water Flow Rates and Travel Times

Despite the better agreement between computed heads and kriged heads in Simulation A-3, Simulation A-2 is considered the more realistic model because it incorporates permeability values for granite wash deposits supported by the presently available data on permeability for the Deep-Basin Brine aquifer (table 2).

Specific discharge rates of ground-water flow may be obtained by dividing the flow rate represented by a streamtube by its width. In addition, pore-fluid velocity is given by dividing specific discharge by porosity. In Simulation A-2 (fig. 12) the model gives values of specific discharge for the shallow section in the range of 3×10^{-4} to 2×10^{-2} m/day and for the deep section of 8×10^{-6} to 10^{-4} m/day. Maximum computed ground-water flow velocity in the Ogallala aquifer is about 1.5×10^{-1} m/day, assuming a porosity of 16 percent (Knowles and others, 1982). In the Deep-Basin Brine aquifer the model indicates maximum ground-water flow velocities in the shelf carbonates of 1.1×10^{-4} m/day and in the proximal granite wash of 4.4×10^{-4} m/day (equivalent to about 400 m and 1,600 m per 10,000 years). Average porosities are assumed to be 8 and 23 percent, respectively, according to Wirojanagud and others (1985). These flow rates are only rough estimates, and more accurate values will depend on acquisition of new, more detailed data on porosity and permeability distribution in the deep section, and on the construction of improved models.

Leakage rate through the evaporite section is only about 6×10^{-8} m/day. Nevertheless, because of its vast area, the evaporite section beneath the High Plains contributes by vertical leakage about 0.0125 m^3/day to the deep aquifer or 27 percent of the water passing through the Deep-Basin Brine aquifer, according to the model (Simulation A-2). The accuracy of this rate is dependent on accuracy of vertical permeability of the aquitard and the head drop across it. In Simulation A-3, computed hydraulic heads in the western part of the deep section are

DRAFT

significantly lower than heads in Simulation A-2. The increase in head drop across the aquitard results in an increase in vertical leakage from 0.0125 m^3/day to 0.0155 m^3/day in Simulation A-3.

Ground-water travel times through the Deep-Basin Brine aquifer from the westernmost recharge area in New Mexico to the eastern boundary of the model (Simulation A-2) range between 1.2 and 4 million years depending on the flow path and average porosities of the different units.

SIMULATION STRATEGY: TRANSIENT MODEL

Realizing the importance of topography on ground-water flow, the modeling in this section is aimed at studying how the ground-water flow pattern has changed as a result of tectonic and geomorphologic events occurring in the Palo Duro Basin during Cenozoic time (table 5). Although little detailed information on timing of the different events is available, the general sequence of events is reasonably well known. Timing of some events may overlap to a certain extent; nevertheless, modeling of the tectonic and geomorphologic processes is performed in successive simulations, using the computed hydraulic head distribution from one simulation as initial conditions for the following simulation. Thus, the modeling results show the effects of individual mechanisms rather than showing the integrated response to several mechanisms.

As discussed earlier, the geometry of the finite element mesh is not changed and only prescribed heads along the surface of the model are varied in order to simulate the change in water table as a result of the modification of topography. Downward propagation of hydraulic head changes at the topographic surface depends on values of hydraulic conductivities and specific storage or the hydraulic diffusivity (K/S_s). Hydraulic conductivity values are the same used in steady-state Simulation A-2. Specific storage was assumed to be uniform at

35

DRAFT

0.0001 m^{-1}. Also, hydrogeologic properties of the individual units are assumed invariant with time.

Approximate steady-state hydrodynamic conditions prior to the uplift of the basin are created in Simulation T-1. The resulting hydraulic head distribution in this simulation is used as initial condition for the subsequent Simulation T-2 describing the uplift and tilting of the basin. Ogallala deposition was modeled in the following Simulation T-3, which in turn uses the computed hydraulic head distribution from Simulation T-2 as initial conditions.

Simulation T-4 investigates the effect of erosion of the Pecos River valley. Prescribed hydraulic heads along the surface nodes representing the Pecos valley area are lowered with time to the approximate present topographic elevation.

In simulation T-5, the latest major erosional event, the westward retreat of the Caprock Escarpment was simulated. Hydraulic heads prescribed to the surface nodes representing the Rolling Plains were lowered in order to mimic the cap-rock retreat.

Additional possible mechanisms creating underpressuring are investigated which include (1) the effect of erosional unloading (Simulation P-1) and (2) the impact of the Panhandle oil and gas field on the hydrodynamics of the Palo Duro Basin (Simulations H-1).

RESULTS AND DISCUSSION

Simulation of Hydrodynamic Development of the Basin

Pre-Uplift Conditions

Pre-uplift conditions are created in Simulation T-1. The boundary conditions in this simulation are represented by prescribed head boundaries along the upper surface with a maximum head difference of 100 m (330 ft) between the western boundary and eastern boundary. McGookey (1984) showed that prior to the uplift the Palo Duro Basin was at or near sea level during Cretaceous time, and no major tectonic events can be identified between

36

DRAF

Cretaceous and Miocene. Accordingly, large hydraulic gradients across the basin are not likely. The computed hydraulic head distribution in figure 20 represents a hypothetical ground-water flow regime prior to uplifting which indicates rather sluggish flow rates with very small hydraulic gradients (less than 2×10^{-4}). However, due to lack of information about the pre-uplift hydrologic system, the simulated flow system represents a rather hypothetical scenario. The uncertainties of this initial model will diminish with subsequent simulations which incorporate more detailed information regarding changes in elevation and topography of the basin.

Basin Uplift and Tilting

The computed hydraulic head distribution was used as initial conditions for Simulation T-2, which investigates the effect of uplift and tilting of the basin on the hydraulic head distribution. Uplift and tilting of the basin was modeled by gradually increasing the hydraulic heads during a time period of one million years along the surface of the mesh relative to the fixed heads along the eastern boundary of the model. The amount of head change increases linearly from 0 meters at the eastern corner to 1,100 m (3,600 ft) at the western boundary in New Mexico. Along the High Plains surface heads increase between 750 m (2,460 ft) in the west and 220 m (720 ft) in the east which corresponds to the range of relative uplift amounts in the Palo Duro Basin (McGookey, 1984).

The computed hydraulic heads in figure 21 show the hydrodynamic conditions 10 million years after the start of uplift. Within the last million years, the maximum change in hydraulic head computed by the model was only 6×10^{-4} m (2×10^{-3} ft), indicating approximate steady-state flow conditions. Hydraulic heads in the Deep-Basin Brine aquifer (fig. 21) are up to 100 m (330 ft) below High Plains surface water table, indicating some underpressuring in the eastern part of the cross section. In the western part, however, hydraulic heads in the deep sections are higher than water-table elevations, indicating the possibility of upward leakage of deep-basinal

37

DRAFT

fluids across the Evaporite aquitard for the time period between uplifting of the basin and erosion of the Pecos River.

To support the approximate steady-state conditions and to test the accuracy of the regional transient simulation, Simulation T-2 was repeated as a steady-state simulation using FREESURF with boundary conditions based on the final prescribed hydraulic heads from Simulation T-2. The computed hydraulic heads in this steady-state simulation (fig. 22) agree well with computed heads in the transient Simulation T-2 (fig. 21). The results indicate that during a time period of less than 9 million years the fluid pressures in the deep section, and also within the Evaporite aquitard, have equilibrated to the modified surface-head boundary conditions (during the first one million years) which represent tectonic uplift and tilting of the basin. Equilibration of hydraulic heads is governed by the hydrologic properties of the different hydrostratigraphic units. Another simulation of basin uplift with increased hydraulic diffusivity of the hydrologic units (that is, either a decrease in hydraulic conductivity, or an increase in specific storage) results in maximum hydraulic head changes of about 2.5 m during the last 1 million years (out of 10 million years), compared to less than 10^{-3} m in the corresponding Simulation T-2. However, the maximum head difference between these two simulations at a particular node location is generally less than 20 m. This relatively small head difference suggests that even with a 10-fold increase in hydraulic diffusivity the resulting head distribution can be approximated with steady-state flow condition. A reduction in hydraulic diffusivity due to a decrease in hydraulic conductivity would affect ground-water flow travel time (10-fold decrease) and thus, the possible ages of the deep basinal fluids.

Deposition of the Ogallala Formation

Deposition of the Ogallala Formation was modeled separately in Simulation T-3, despite the fact that uplifting and Ogallala deposition are probably overlapping events. Hydraulic heads along the topographic surface boundary are increased 50 m (165 ft) in the east and up to 125 m (430 ft) in the west accounting for a general decrease in thickness of the Ogallala away from

38

the sediment source to the west of the model. Along the High Plains surface, prescribed hydraulic heads were adjusted to the computed water table from the steady-state Simulation A-2 (fig. 12). Again, prescribed heads along the upper surface are gradually increased during a time period of one million years. The computed hydraulic head distribution in Simulation T-3 (fig. 23) describes the hydrodynamic condition 10 million years after the beginning of the Ogallala deposition.

Although prescribed heads along the High Plains surface increased by up to 125 m (410 ft), hydraulic heads in the Deep-Basin Brine aquifer generally increase by less than 70 m (230 ft). Thus, deposition of the Ogallala and the resulting increase in water table contributed to the apparent underpressuring in the deep section. Tóth and Millar (1983), who investigated vertical propagation of hydraulic head changes through thick low-permeability strata, showed that fluid pressures at great depths may survive changes in topography and be in a transient state for hundreds to millions of years. It is useful to compare the model results with the hydraulic head response for a uniform one-dimensional system similar to the example performed in Tóth and Miller (1983), using the following equation:

$$\frac{\partial}{\partial z}\left(K_z \frac{\partial h}{\partial z}\right) = S_s \frac{\partial h}{\partial t}$$

where K_z is the vertical hydraulic conductivity, S_s is the specific storage, and h is the hydraulic head. Computation of vertical hydraulic head dissipation across 1,500 m (4,920 ft) thick aquitard ($K_v = 3.2 \times 10^{-7}$ m/day and $S_s = 10^{-4}$ 1/m) results in 75 percent equilibration of hydraulic heads at 1,500 m depth after 9 million years. Accordingly, an instant head increase of 125 m at the upper surface would result in a head increase of more than 94 m at the base of the maximal 1,500 m thick Evaporite aquitard by vertical dissipation of hydraulic heads. Toward the eastern part of the basin the thickness of the Evaporite aquitard decreases and hydraulic heads at depth would equilibrate more rapidly to changes at the upper surface. Although the discrepancy in the hydraulic-head response in Simulation T-3 and those calculated assuming a uniform one-dimensional system is not very large considering the uncertainities in hydrologic

39

properties, the fact that the computed hydraulic heads in Simulation T-3 are approximately at steady-state, suggests a complete equilibration of hydraulic heads in the system in response to the head changes imposed along the upper surface. This indicates that the lateral flow component within the deep aquifer is important in equilibrating hydraulic head changes along the topographic surface, and furthermore, in creating underpressured conditions in the deep aquifer.

Erosion of the Pecos River

The importance of the Pecos River on underpressuring in the western part of the Deep-Basin Brine aquifer was demonstrated in the previous section (fig. 19). In Simulation T-4, prescribed heads along the surface nodes representing the Pecos River valley are gradually lowered during a time period of 4 million years. At the end of the time period, the heads along the surface of the mesh correspond to the approximate present-day water table which roughly follows the topography.

Figure 24 shows a significant reduction of hydraulic heads in the western part of the Deep-Basin Brine aquifer 5 million years after the start of the stream erosion. The maximum change in hydraulic heads during the last one million years of the simulation was about 1.7 m (5.6 ft), indicating that overall steady-state flow conditions can be assumed at the end of the simulation. Underpressuring in the deep section is indicated by the difference in hydraulic head between the shallow aquifer and the deep section. This difference increases from a maximum of 125 m (410 ft) in Simulation T-3 (fig. 20) to a maximum of 175 m (575 ft) in this simulation (fig. 24).

The impact of the Pecos River erosion on the hydraulic head distribution is documented in figure 25, which shows the difference in heads before and after stream erosion. The head change decreases away from the Pecos with less than 25 m (82 ft) of change occurring east of

40

DRAF

the Caprock Escarpment. Westward retreat of the Caprock Escarpment has a similar effect on the ground-water flow system as will be shown below.

Erosion of the Eastern Caprock Escarpment

The effect of westward retreat of the Caprock Escarpment on the hydrologic conditions in the Palo Duro Basin was investigated in Simulation T-5. Prescribed hydraulic heads along the surface nodes located at the present-day Rolling Plains surface were reduced to simulate the erosion of the High Plains according to the reported maximum rate of cap-rock retreat of 18 cm/yr (7.1 inches/year). At the "end of the cap-rock retreat" (about 1.1 million years), hydraulic heads along the surface of the model correspond to the modern water-table configuration along the cross-sectional traverse. Hydraulic heads along the eastern boundary of the mesh are lowered simultaneously with the decline in water table at the surface (during a time period of 100,000 years), maintaining predominantly horizontal flow along the eastern boundary. Pressure-depth data from the deep section in the Hardeman Basin, located approximately at the eastern edge of the cross section, indicate roughly hydrostatic conditions (fig. 10).

Permian and Pennsylvanian formations crop out along the Wichita Mountains in Oklahoma about 100 km (62 mi) from the eastern edge of the cross section. Erosion of the High Plains in that area and resulting subareal exposure of the deep aquifers is assumed to create predominantly horizontal hydraulic gradients in the deep aquifers, as observed today. Thus, the assumption of horizontal flow at the eastern boundary of the model appears reasonable. It is conceivable that heads in the deep section decrease prior to the water-level drop at the surface as a result of equilibration with relatively lower heads in the outcrop area further to the east, where water levels decrease earlier than those at the eastern boundary of the model. The impact of possible lag in head decline in the deep section along the eastern boundary of the model is considered small and certainly does not change the resulting hydrodynamic conditions in the simulation.

41

DRAFT

Computed hydraulic heads in Simulation T-5 (fig. 26), representing the hydrodynamic conditions after 1.1 million years, show a significant drop in hydraulic heads in the deep section. Underpressuring (head difference between water table and deep section) increases from about 175 m (575 ft) in Simulation T-4 (fig. 24) to more than 350 m (1,150 ft) in this simulation (fig. 26). The impact of cap-rock retreat on the hydrologic regime is shown in figure 27. In the deep section, greatest change in hydraulic head of up to 250 m (820 ft) occurred beneath the present-day escarpment. Toward New Mexico, the head difference decreases, indicating diminished influence of cap-rock retreat on the hydraulic heads. These results indicate a significant effect on the overall ground-water flow pattern in the deep section within the last one to two million years. These changes in hydraulic gradients and ground-water flow paths result in changes in residence time of fluids in the basin. Also, transport of chemical constituents could have travelled along ancient pathways much different than is suggested by the present-day hydraulic-head distribution. This could be an important factor with regard to the chemical evolution of deep basinal brines.

Maximum computed head changes within the last 100,000 years of Simulation T-5 was about 3.2 m (10.5 ft), which suggests that during the recent geologic history, hydraulic heads were still equilibrating slightly to the modified hydrologic boundary conditions created by the westward retreat of the Caprock Escarpment. Computed hydraulic head distribution in Simulation T-5 (fig. 26) agrees reasonably well with the equivalent steady-state Simulation A-2 shown in figure 12, indicating that the present-day hydraulic head distribution in the basin can be assumed to represent approximate steady-state flow conditions.

The importance of good hydrologic connection (granite wash) between the area beneath the High Plains and the relatively lower hydraulic heads along the eastern boundary has been documented earlier in the steady-state simulations. In order to evaluate the significance of only the water-level decline along the present-day Rolling Plains surface, two additional transient simulations were run. The two simulations correspond to Simulation T-4 and T-5, whereby the first simulation (Pecos River erosion) incorporated reduced prescribed heads of

42

DRAFT

430 m (1,410 ft) in the deep brine aquifer along the eastern boundary. The computed head distribution of this modified simulation yielded hydraulic heads that were lower in the central part of the deep brine aquifer by up to 120 m (395 ft) as compared to Simulation T-4.

Subsequent simulation of the westward retreat of the Caprock Escarpment was performed, whereby only the prescribed heads along the present-day Rolling Plains surface were decreased, and which used the results from the modified Simulation T-4 (Pecos River erosion with artificially reduced prescribed heads along the eastern boundary) as initial conditions. This second simulation yielded a general decrease in hydraulic heads in the central part of the deep aquifer by up to 130 m (430 ft). The overall hydraulic head distribution from this simulation compared closely with the results of Simulation T-5.

The decrease in hydraulic heads of 120 m and 130 m, respectively, has about the same magnitude, which indicates that both the reduction in hydraulic heads along the eastern boundary and the water-table decline along the surface as a result of the cap-rock retreat are equally important for creating significant underpressuring in the Deep-Basin Brine aquifer. The thinning of the evaporite sequence toward Oklahoma and the assumed relatively higher permeability of the Permian mud-flat system (fig. 4) allows for propagation of reduced hydraulic heads at the surface (as a result of the drop in topography) into the deeper aquifer system.

Effect of Erosional Unloading

Erosion and the resulting unloading of underlying formations has been suggested as a cause of significant underpressuring under appropriate conditions (Ferran, 1972; Fertl, 1976; Neuzil and Pollock, 1983). Erosional unloading could result in dilation of clayey material causing reduced pore pressures (fig. 3). Fluids from the adjacent aquifer could flow into the shale sections creating reduced hydraulic heads in the surrounding aquifer (Ferran, 1972). Neuzil and Pollock (1983) documented the potential underpressuring in relatively tight formations for a one-dimensional case. In general, the extent of underpressuring depends on the rate of erosion

43

DRAFT

and the hydraulic diffusivity which takes into account the coefficient of compressibility of the material.

The westward retreat of the Caprock Escarpment represents a removal of up to 300 m (1,000 ft) of overburden. Assuming that primarily the underlying aquitard is capable of volume expansion, subhydrostatic conditions can be created within the aquitard. The results could be hydraulic gradients inward toward the center of the aquitard thereby modifying the overall downward gradients. However, erosion of the "High Plains" occurs laterally, indicating that erosional unloading affects the underlying formations only in the vicinity of the location of the Caprock Escarpment. After the position of the escarpment retreats further to the west, the effect of erosional unloading ceased and possible subhydrostatic pressures within the aquitard could then equilibrate with hydrostatic heads at the surface.

The possible impact of erosional unloading on the hydraulic heads will be investigated in Simulation P-1. For this purpose, the simulation describing the westward retreat of the eastern Caprock Escarpment (Simulation T-5) is repeated; this time, however, the potential decompaction of the underlying aquitard unit is incorporated into the cross-sectional model. The equation describing two-dimensional ground-water flow in vertically deformable media is given by Jacob (1950):

$$\frac{\partial}{\partial x}(K_x\frac{\partial h}{\partial x}) + \frac{\partial}{\partial z}(K_z\frac{\partial h}{\partial z}) = S_s\frac{\partial h}{\partial t} - \alpha\frac{\partial \sigma}{\partial t}$$

where K_x and K_z are the horizontal and vertical hydraulic conductivities, S_s is the specific storage, α is the coefficient of compressibility of the solid, σ is the total stress, and h is the hydraulic head. Without the term $\alpha\frac{\partial \sigma}{\partial t}$ accounting for the changes in pore volume due to change in vertical stress, this equation is the well-known ground-water flow equation which is solved numerically by the computer program FLUMPS described earlier.

The technique for simulating the effect of erosional decompaction using the general ground-water flow algorithm in the program FLUMPS involves the treatment of the mathe-

44

matical term describing the vertical deformation of the media similar to a source-sink term in the normal two-dimensional, transient ground-water flow equation (Jacob, 1950; Bredehoeft and Cooley, 1983; Narasimhan and Kanehiro, 1980). Thus, if one knows or can assume values of α and $\frac{\partial \sigma}{\partial t}$, the stress term can be added as a source-sink term in the program. Accordingly, necessary information includes vertical compressibility of the aquitard material, and the weight of overburden that is removed over a particular time interval. It is assumed that the weight that is removed as a result of the cap-rock retreat is the same at each location. Further, typical values are assumed for consolidated clay compressibility of 10^{-8} m^2/N, and specific weight of the removed material of 2.72 g/cm^3. Although the Evaporite aquitard contains only a fraction of clay, this compressibility value translates to a value of specific storage of about 10^{-4} m^{-1} (neglecting the compressibility of the fluid) that has been used in this study for the different hydrologic units.

Simulation P-1 (fig. 28) shows the hydraulic head distribution at a time of 800,000 years after the start of the caprock retreat from the eastern edge of the cross-sectional model. The head distribution in the shallow aquitard section shows local underpressured conditions in the vicinity of the temporary location of the caprock. However, further to the east, hydraulic heads in the aquitard are already largely equilibrated to approximate hydrostatic conditions. With continued retreat of the Caprock Escarpment, the local zone of underpressuring moves westward indicating that underpressured conditions may occur within the aquitard under the present-day location of the escarpment. However, lower values of aquitard compressibility would reduce this effect significantly.

It is important to note that this simulation represents a hypothetical scenario as underpressuring in the shallow aquitard section has not been confirmed, mainly because of lack of measurements. However, the described mechanism is likely to occur and the extent of the underpressuring depends largely on the hydraulic diffusivity and the rate of erosion (Neuzil and Pollock, 1983). Investigation of shale transit times based on geophysical logs might give an

45

DRAFT

indication of possible decompaction of shale units in the vicinity of the Caprock Escarpment and could be used to support the proposed mechanism (Magara, 1976).

The results of this simulation also have implications on the shallow ground-water flow system in the vicinity of the caprock. As shown in figure 28, the expanding aquitard unit acts as a hydrologic sink creating a significant hydraulic gradient toward the center of the aquitard. This represents a strong driving force for shallow ground-water to penetrate great depths within the aquitard section and enhance salt dissolution processes which in turn causes fracturing and collapse of overlying units. The result would be an increase in overall aquitard permeability and dissipation of subhydrostatic heads within the aquitard. Thus, the potential extent of underpressuring would be reduced with time as a result of salt dissolution phenomena.

Effect of Hydrocarbon Production

To determine if oil and gas production from the Panhandle oil and gas field, which is located along the northern boundary of the Palo Duro Basin, would affect the potentiometric surface of the Deep-Basin Brine aquifer on a regional scale, the effect of reservoir pressure drop on the hydrodynamics of the aquifer was tested in Simulation H-1. According to field data, reservoir pressures in the Panhandle oil and gas field over the Amarillo Uplift had dropped approximately 2.76 MPa (400 psi) before water injection was started to enhance oil and gas recovery.

Effects of hydrocarbon production were simulated by gradually reducing prescribed hydraulic heads at two node locations representing a hypothetical reservoir in the cross-sectional model. The distance between the center of the cross-sectional model and the location of the selected "reservoir" nodes east of the escarpment corresponds to the distance between the center of the Palo Duro Basin and the Panhandle oil and gas field to the north of the basin and, therefore, provide a reasonable scenario for the effect of hydrocarbon production from the Panhandle field on the hydrodynamic conditions in the rest of the basin. There are no known oil or gas fields in the central part of the Palo Duro Basin.

46

DRAFT

Hydraulic heads at the two "reservoir" nodes were gradually decreased from the initial head values computed in the previous simulation by about 200 m which corresponds to a drop in reservoir pressure of about 400 psi during a time period of 50 years after which prescribed heads were kept constant for another 50 years. The computed head distribution (fig. 28) indicates that the effect of reservoir-pressure drop is restricted to the immediate vicinity of the reservoir and does not affect the overall ground-water flow pattern in the deep section.

In a subsequent simulation, the prescribed head boundary conditions at the particular "reservoir" nodes were removed to investigate how long it would take to reach the original head distribution prior to the pressure drop caused by hydrocarbon production. After 1,000 years, hydraulic heads at the "reservoir" nodes had recovered 75 percent to the original heads, and after 10,000 years hydraulic heads had recovered 90 percent.

In general, potentiometric surface maps for the deeper hydrologic units are based on pressure data from drill-stem tests and should not incorporate data from oil fields that indicate depressured conditions, because depressuring is restricted to local areas and does not reflect regional fluid pressure distribution. Performance assessment analyses for the migration of radionuclides from a nuclear waste repository are generally developed for scenarios of 10,000 years or longer. Depressured oil fields impact only localized areas and should have equilibrated within 10,000 years. Therefore, these local depressured reservoirs along the borders of the Palo Duro Basin should not significantly alter the regional ground-water flow pattern beneath the High Plains. Further, the local extent of the pressure depletion is suggested by the fact that most reservoirs in the Panhandle oil and gas field have either depletion-drive or solution-gas drive which indicates that these reservoirs are hydraulically isolated from fluid pressures in the surrounding formations.

In contrast, simulating the effects of hydrocarbon production assumed that the reservoir has a strong water-drive indicating that the reservoir is hydraulically connected to the regional hydrodynamic regime. This is supported by Hubbert (1967), who identified a hydrodynamic component responsible for the entrapment of the Panhandle oil and gas field which would

47

suggest some hydraulic interconnection with the regional ground-water flow. Wirojanagud and others (1984) implied in their ground-water flow model that ground water in the Wolfcamp aquifer could flow across the northwestern part of the Amarillo Uplift, which suggests hydraulic connection of the hydrocarbon reservoir on the uplifted formations with the regional hydro-dynamics. Nevertheless, the results of the simulation suggest that only in the immediate vicinity of the depleted oil reservoir are the hydraulic heads affected.

SUMMARY

A regional ground-flow model along an east-west cross section through the Palo Duro Basin was constructed. In the first phase of the study, in which steady-state ground-water flow was simulated, the effects of topography and hydrostratigraphy on the regional ground-water flow regime were investigated. In the second phase, long-term transient flow conditions caused by tectonic and geomorphologic processes were investigated.

Characterization of the regional ground-water flow in the Palo Duro Basin, based on results from the steady-state ground-water flow model, can be summarized as follows: distinction of a shallow flow system governed primarily by topography, and a deeper flow regime recharging in the New Mexico area and passing deep beneath the Pecos River into the deep section of the Palo Duro Basin (fig. 4).

The observed underpressuring in the Deep-Basin Brine aquifer underlying the High Plains surface can be explained by the regional topography and geology. Specifically, the Ogallala water table is relatively high due to the elevation of the High Plains; the potentiometric surface of the Deep-Basin Brine aquifer is relatively low due to the draining effect of permeable granite-wash strata and very low recharge water; and the low-permeability Evaporite aquitard effectively segregates the two aquifer systems, thereby maintaining the large head differential. The model also indicated that the Pecos River enhances under-

48

DRAFT

pressuring beneath the western half of the High Plains by serving as a discharge area for some of the ground water that would otherwise move downdip into the Deep-Basin Brine aquifer.

Poor hydraulic connection (low K_v) between the Ogallala and Dockum aquifers affects the amount of leakage through the Evaporite aquitard by restricting the amount of recharge reaching the top of the aquitard. Information on the vertical hydraulic gradient in the units overlying the salt section is needed to more accurately model leakage through the evaporite section.

Investigation of the hydrodynamic development of the Palo Duro Basin by means of transient modeling indicates that uplift and tilting of the basin caused increased flow rates in the Palo Duro Basin about 10 to 15 million years ago. Erosion of the Pecos River valley and the more recent retreat of the Caprock Escarpment in combination with the draining effect of the relatively permeable granite-wash deposits contribute to the observed underpressuring in the Deep-Basin Brine aquifer.

The westward retreat of the Caprock Escarpment, which results in a drop in water table in the shallow aquifer, significantly affects the hydraulic heads in the deep section (head decline of up to 250 m in the deep section). The model shows that because of the relatively permeable granite wash in the eastern part of the cross section (proximal deposits), hydraulic heads beneath the evaporite sequence can adjust more readily to the lower hydrostatic heads at the eastern boundary of the model than to the higher heads of the High Plains aquifer.

Results of Simulation T-5 (retreat of the Caprock Escarpment) imply that up to 250 m of underpressuring observed beneath the Evaporite aquitard occurred within the last one to two million years as a result of the cap-rock retreat. The resulting change of hydraulic head distribution during that period suggests a significant effect on the overall ground-water flow pattern in the deep section within the last one to two million years. This could be an important factor with regard to the chemical evolution of deep basinal brines. The change in hydraulic gradient and ground-water flow pattern can significantly affect the residence time of deep-

49

DRAFT

basinal brines. Further, transport of chemical constituents could have traveled along ancient pathways much different than is suggested by the present-day hydraulic-head distribution.

The modeling effort also suggested that erosional unloading in connection with the retreat of the Caprock Escarpment can be considered ineffective in creating large-scale underpressuring in the Deep-Basin Brine aquifer or in significantly altering flow direction within the aquitard for long periods of time. Only in the direct vicinity of the escarpment it is possible that erosional unloading could create significant underpressuring in the underlying aquitard. Similarly hydrocarbon production and the concomitant reduction in reservoir pressure affect hydraulic heads only locally and do not influence the regional ground-water flow regime in the Deep-Basin Brine aquifer.

DRAFT

REFERENCES

Bassett, R. L., and Bentley, M. E., 1982, Geochemistry and hydrodynamics of the deep formation brines in the Palo Duro and Dalhart Basins, Texas, USA: Journal of Hydrology, v. 59, p. 331-372.

Bassett, R. L., Bentley, M. E., and Simkins, W. W., 1981, Regional ground-water flow in the Panhandle of Texas: a conceptual model, in Gustavson, T. C., and others, Geology and geohydrology of the Palo Duro Basin, Texas Panhandle -- a report on the progress of nuclear waste isolation feasibility studies (1980): The University of Texas at Austin, Bureau of Economic Geology Geological Circular 81-3, p. 102-107.

Bell, J. S., and Shephard, J. H., 1951, Pressure behavior in the Woodbine Sand: American Institute of Mining, Metallurgical, and Petroleum Engineers, Petroleum Transactions, v. 192, p. 19-28.

Bergren, W. A., and Van Convering, J. A., 1974, The Late Neogene: Amsterdam, Elsevier, v. 16, no. 1/2, 228 p.

Bradely, J. S., 1975, Abnormal formation pressure: American Association of Petroleum Geologists Bulletin, v. 59, no. 6, p. 957-973.

Bredehoeft, J. D., and Hanshaw, B. B., 1968, On the maintenance of anomalous fluid pressures, 1. Thick sedimentary sequences: Geological Society of America Bulletin, v. 79, p. 1097-1106.

Bredehoeft, J. D., and Cooley, R. L., 1983, Comment on "A Note on the Meaning of Storage Coefficient" by T. N. Narasimhan and B. Y. Kanehiro: Water Resources Research, v. 19, no. 6, p. 1632-1634.

Conti, R. D., Herron, M. J., Senger, R. K., and Wirojanagud, P., 1984, Stratigraphy and influence of porosity on ground-water flow in the Wolfcamp Brine aquifer, Palo Duro

DRAFT

Basin, Texas Panhandle: The University of Texas at Austin, Bureau of Economic Geology Open-File Report OF-WTWI-1985-19.

Core Laboratories, Inc., 1972, A survey of the subsurface saline water of Texas, v. 3. Aquifer rock properties: Texas Water Development Board Report 157, 364 p.

Davis, S. N., 1980, Hydrogeologic effects of natural disruptive events on nuclear waste repositories: Pacific Northwest Lab., Research Report No. PNL-2858, 33 p.

Davis, S. N., and DeWiest, R. J., 1966, Hydrogeology: New York, John Wiley, 463 p.

Dickey, P. A., and Cox, W. C., 1977, Oil and gas in reservoirs with subnormal pressures: American Association of Petroleum Geologists Bulletin, v. 61, no. 12, p. 2134-2142.

Domenico, P. A., and Mifflin, M. D., 1965, Water from low permeability sediments and land subsidence: Water Resources Research, v. 1, no. 4, p. 563-576.

Dutton, A. R., 1985, Hydrologic testing in the salt dissolution zone of the Palo Duro Basin, Texas Panhandle: The University of Texas at Austin, Bureau of Economic Geology Open-File Report OF-WTWI-1985-33.

Dutton, A. R., and Orr, E. D., 1985, Hydrogeology and hydrochemical facies of the San Andres Formation in eastern New Mexico and the Texas Panhandle: The University of Texas at Austin, Bureau of Economic Geology Open-File Report OF-WTWI-1985-2.

Dutton, A. R., and Simpkins, W. W., 1985, Hydrogeology and water resources of the Lower Dockum Group (Triassic) in the Texas Panhandle and eastern New Mexico: The University of Texas at Austin, Bureau of Economic Geology Open-File Report OF-WTWI-1985-32.

Dutton, S. P., Goldstein, A. B., and Ruppel, S. C., 1982, Petroleum potential of the Palo Duro Basin, Texas Panhandle: The University of Texas at Austin, Bureau of Economic Geology Report of Investigations No. 123, 87 p.

Ferran, D. M., 1973, Evaluation of abnormally high- and low-pressured Morrow sands in northwestern Oklahoma using well logs and water sample data: Master's thesis, University of Tulsa, 110 p.

DRAFT

Fertl, W. H., 1976, Abnormal formation pressures: implications to exploration, drilling, and production of oil and gas resources: New York, Elsevier.

Fink, B. E., 1963, Ground-water geology of Triassic deposits, northern part of the Southern High Plains of Texas: High Plains Underground Water Conservation District No. 1, Report No. 163, 79 p.

Fisher, R. S., and Kreitler, C. W., in preparation, Hydrochemistry of Palo Duro brines, in Gustavson, T. C., and others, Geology and hydrogeology of the Palo Duro Basin, Texas Panhandle, a report on the progress of nuclear waste isolation feasibility studies (1983): The University of Texas at Austin, Bureau of Economic Geology Geological Circular.

Fogg, G. E., and Senger, R. K., 1985, Automatic generation of ground-water flow nets using numerical models: Ground Water, v. 23, no. 3, p 336-344.

Freeze, R. A., and Cherry, J. A., 1979, Ground water: Englewood Cliffs, N.J., Prentice Hall, 604 p.

Gies, R. H., 1985, Case history for a major Alberta Basin gas trap: the Cadomin Formation, in Elmworth, Case study of a deep basin gas field: American Association of Petroleum Geologists Memoir 38, p. 115-140.

Gross, G. W., Hoy, R. N., Duffy, C. J., and Rehfeldt, K. R., 1982, Isotope studies of recharge in the Rosswell Basin, in Perry, E. C., Jr., and Montgomery, C. W., eds., Isotopic studies of hydrologic processes: Dekalb, Illinois, Northern Illinois University Press, p. 25-33.

Gustavson, T. C., Finley, R. J., and Baumgardner, R. W., Jr., 1981, Retreat of the Caprock Escarpment and denudation of the Rolling Plains in the Texas Panhandle: Bulletin of the Association of Engineering Geologists, v. 18, no. 4, p. 413-422.

Handford, C. R., 1980, Lower Permian facies of the Palo Duro Basin, Texas: depositional systems, shelf-margin evolution, paleogeography, and petroleum potential: The University of Texas at Austin, Bureau of Economic Geology Report of Investigations No. 102, 31 p.

DRAFT

Handford, C. R., and Dutton, S. P., 1980, Pennsylvanian-Lower Permian depositional systems and shelf-margin evolution, Palo Duro Basin, Texas: American Association of Petroleum Geologists Bulletin, v. 64, no. 1, p. 88-106.

Handford, C. R., Presley, M. W., and Dutton, S. P., 1980, Depositional and tectonic evolution of a basement-bounded, entracratonic basin, Palo Duro Basin, Texas (abs.): AAPG Bulletin, v. 64, p. 717.

Handford, C. R., Dutton, S. P., and Fredericks, P. E., 1981, Regional cross sections of the Texas Panhandle: Precambrian to Mid-Permian: The University of Texas at Austin, Bureau of Economic Geology Cross Sections.

Hubbert, M. K., 1940, The theory of ground-water motion: Journal of Geology, v. 48, p. 785-944.

_____ 1967, Application of hydrodynamics to oil exploration: 7th World Petroleum Congress Proceedings, Mexico City, v. 1B, p. 59-75.

INTERA, 1983, First status report on regional ground-water flow modeling for the Palo Duro Basin, Texas: ONWI/E512-02900/TR-13.

Izeet, G. A., Obradovich, J. D., Naeser, C. W., and Cebula, G. T., 1981, Potassium-argon and fission-track zircon ages of Cerro Toledo Rhyolite tephra in the Jemer Mountains, north-central New Mexico: U.S. Geological Survey, Professional Paper 1199D, p. 32-43.

Izeet, G. A., Wilcox, R. E., and Borchart, G. A., 1972, Correlation of a volcanic ash bed in Pleistocene deposits near Mt. Blanco, Texas, with the Guaje pumice bed of the Jemer Mountains, New Mexico: Quarternary Research, v. 2, p. 554-578.

Jacob, C. E., 1950, Flow of ground water, in Rouse, H. (ed.), Engineering Hydraulics, p. 321-386, John Wiley, New York.

Knowles, T., Nordstrom, P., and Klemt, W. B., 1982, Evaluating ground water resources of the High Plains, Final Report: Texas Department of Water Resources, LP-173.

Kreitler, C. W., and Bassett, R. L., 1983, Chemical and isotopic composition of saline ground water and saline springs in the Rolling Plains east of the Ogallala Escarpment, in

54

DRAFT

Gustavson, T. C., and others, Geology and geohydrology of the Palo Duro Basin, Texas Panhandle, a report on the progress of nuclear waste isolation feasibility studies (1982): The University of Texas at Austin, Bureau of Economic Geology Geological Circular 83-4, p. 116-124.

Kreitler, C. W., Fisher, R. S., Senger, P. K., Hovorka, S. D., Dutton, A. R., 1984, Hydrology of an evaporite aquitard: Permian Evaporite: The University of Texas at Austin, Bureau of Economic Geology Open-File Report OF-WTWI-1984-52.

Law, B. E., and Dickinson, W. W., 1985, Conceptual model for origin of abnormally pressured gas accumulations in low-permeability reservoirs: American Association of Petroleum Geologists Bulletin, v. 68, no. 8, p. 1295-1304.

Magara, K., 1976, Thickness of removed sediments, paleopore pressure, and paleotemperature, southwestern part of Western Canadian Basin: American Association of Petroleum Geologists Bulletin, v. 60, p. 554-565.

McGookey, D. A., 1984, Uplift, tilting, and subsidence of the Palo Duro Basin area: The University of Texas at Austin, Bureau of Economic Geology Open-File Report OF-WTWI-1984-2.

McGowen, J. H., 1981, Depositional sequences and associated sedimentary diagenetic facies: an ongoing investigation of salt-bearing core, Swisher County, Texas, in Gustavson, T. C., and others, Geology and geohydrology of the Palo Duro Basin, Texas Panhandle, a report on the progress of nuclear waste isolation feasibility studies (1980): The University of Texas at Austin, Bureau of Economic Geology Geological Circular 81-3, p. 90-92.

McGowen, J. H., Granata, G. E., and Seni, S. J., 1979, Depositional framework of the lower Dockum Group (Triassic), Texas Panhandle: The University of Texas at Austin, Bureau of Economic Geology Report of Investigations No. 97, 60 p.

Mower, R. W., Hood, J. W., and Cushman, R. L., 1964, An appraisal of potential ground water salvage along the Pecos River between dome and artesia: U. S. Geological Survey Water Supply Paper 1659.

55

DRAFT

Myers, B. N., 1969, Compilation of results of aquifer tests in Texas: Texas Water Development Board Report No. 98, 532 p.

Narasimhan, T. M., Neuman, S. P., and Witherspoon, P. A., 1977, Mixed explicit-implicit iterative finite element scheme for diffusion type problems, II, solution strategy and examples: International Journal for Numerical Methods in Engineering, v. 11, p. 325-344.

Narasimhan, T. N., Neuman, S. P., and Witherspoon, P. A., 1978, Finite element method for subsurface hydrology using a mixed explicit-implicit scheme: Water Resources Research, v. 14, no. 5, p. 863-877.

Narasimhan, T. N., and Kanehiro, B. Y., 1980, A note on the meaning of storage coefficient: Water Resources Research, v. 16, no. 2, p. 423-429.

Neuman, S. P., 1979, User's guide for FLUMPS: Tucson, Arizona, Department of Hydrology and Water Resources, University of Arizona.

Neuman, S. P., Preller, C., and Narasimhan, T. N., 1982, Adaptive explicit-implicit quasi three-dimensional finite element model of flow and subsidence in multiaquifer systems: Water Resources Research, v. 18, no. 5, p. 1551-1561.

Neuman, S. P., and Witherspoon, P. A., 1970, Finite element method of analyzing steady seepage with a free surface: Water Resources Research, v. 6, no. 3, p. 889-897.

Neuzil, C. E., and Pollock, D. W., 1983, Erosional unloading and fluid pressures in hydraulically "tight" rocks: Journal of Geology, v. 91, no. 2, p. 179-193.

Nicholson, J. H., 1960, Geology of the Texas Panhandle, in Aspects of the Geology of Texas: a symposium: University of Texas, Austin, Bureau of Economic Geology Publication 6017, p. 51-64.

Orr, E. D., and Kreitler, C. W., 1985, Interpretation of pressure-depth data from confined underpressured aquifers exemplified by the Deep-Basin Brine aquifer, Palo Duro Basin, Texas: Water Resources Research, v. 21, no. 4, p. 533-544.

DRAFT

Richter, B. C., 1983, Geochemical and hydrogeological characteristics of salt springs and
shallow subsurface brines in the Rolling Plains of Texas and southwest Oklahoma: The
University of Texas at Austin, Master's thesis, 147 p.

Russell, W. L., 1972, Pressure-depth relations in the Appalachian region: American Association
of Petroleum Geologists Bulletin, v. 56, no. 3, p. 528-536.

Senger, R. K., and Fogg, G. E., 1983, Regional modeling of ground-water flow in the Palo Duro
Basin, Texas Panhandle, in Gustavson, T. C., and others, Geology and geohydrology of the
Palo Duro Basin, Texas Panhandle, a report on the progress of nuclear waste isolation
feasibility studies (1982): The University of Texas at Austin, Bureau of Economic Geology
Geological Circular 83-4, p. 109-115.

Seni, S. J., 1980, Sand-body geometry and depositional systems, Ogallala Formation, Texas: The
University of Texas at Austin, Bureau of Economic Geology Report of Investigations
No. 105, 35 p.

Siminitz, P. C., 1985, Hydrogeologic subdivision of the Wolfcamp Series and Pennsylvanian
System of Eastern New Mexico: Stone & Webster Engineering Corporation, Topical
Report, ONWI/SUB/85, E512-05000-T41.

Smith, D. A., 1983, Permeability of the Deep-Basin Brine aquifer system, Palo Duro Basin, in
Gustavson, T. C., and others, Geology and geohydrology of the Palo Duro Basin, Texas
Panhandle, a report on the progress of nuclear waste isolation feasibility studies (1982):
The University of Texas at Austin, Bureau of Economic Geology Geological Circular 83-4,
p. 89-93.

Smith, D. A., Akhter, M. S., and Kreitler, C. W., 1985, Ground-water hydraulics of the Deep-
Basin Brine aquifer system, Palo Duro Basin, Texas Panhandle: The University of Texas at
Austin, Bureau of Economic Geology Open-File Report OF-WTWI-1985-16.

SWEC, 1983, Hydrogeologic investigations based on Drill-Stem Test data, Palo Duro Basin area
and New Mexico: Stone & Webster Engineering Corporation, Topical Report,
ONWI/SUB/83, E512-05000-T14.

Tedford, R. H., 1981, Mammalian biochronology of the late Cenozoic basins of New Mexico: Geological Society of America Bulletin, Part 1, v. 92, p. 1008-1022.

Thomas, R. G., 1972, The geomorphic evolution of the Pecos River system: Waco, Texas, Baylor University, Baylor Geological Studies Bulletin 22, 31 p.

Tóth, J., and Millar, R. F., 1983, Possible effects of erosional changes of the topographic relief on pore pressures at depth: Water Resources Research, v. 19, no. 6, p. 1585-1597.

Tóth, J., 1978, Gravity-induced cross-formational flow of formation fluids, Red Earth Region, Alberta, Canada: analysis, patterns, and evolution: Water Resources Research, v. 14, no. 5, p. 805-843.

Warren, J. E., and Price, H. S., 1961, Flow in heterogeneous porous media: Society of Petroleum Engineers, v. 1, p. 153-169.

Wirojanagud, P., Kreitler, C. W., and Smith, D. A., 1985, Numerical modeling of regional ground-water flow in the Deep-Basin Brine aquifers of the Palo Duro Basin, Texas Panhandle: The University of Texas at Austin, Bureau of Economic Geology Open-File Report OF-WTWI-1984-8.

DRAFT

Appendix A

Effect of Node Spacing Differences in Horizontal
and Vertical Direction on the Hydraulic Head Solution

Anisotropic node spacing in numerical models can cause significant numerical errors in the solution of hydraulic head. Typical horizontal and vertical node spacings in the present model are 12,300 m (40,350 ft) and 250 m (820 ft), respectively. To test the effects of anisotropic node spacing on hydraulic heads computed by the program "FREESURF," several numerical experiments were run.

Finite element grids were set up with 4, 50, 100, and 200 elements with each mesh having the same total size. Each finite element mesh consists of three columns of nodes and each is subdivided horizontally to obtain 4, 5, 100, or 200 elements in successive simulations (fig. A1).

The boundary conditions of the model are such tat the upper left node #3 has a prescribed head of 100 m (330 ft), and the lower right node #7 has a prescribed head of 0 m (0 ft). Boundary conditions on all other nodes are no-flow (prescribed flux equal to zero). The finite difference grid has a total size of 5,000 m (16,400 ft) in horizontal direction and 2,500 m (8,200 ft) in vertical direction. The size for each individual element for the various cases ranges from 2,500 m (8,200 ft) x 1,250 m (4,100 ft) (4-element case), 2,500 m (8,200 ft) x 100 m (330 ft) (50-element case), 2,500 m (8,200 ft) x 50 m (165 ft) (100-element case) to 2,500 m (8,200 ft) x 25 m (82 ft) (200-element case).

The hydraulic head distribution was simulated under two different hydrologic conditions:

1. isotropic, homogeneous conditions with $K_x = K_y = 30$ m/day

2. anisotropic, homogeneous conditions with $K_x = 30$ m/day and $K_y = 3,000$ m/day

The difference in horizontal and vertical node spacing affects the conductance term (C), which represents the rate of fluid transfer due to a unit difference in hydraulic head between two nodes:

$$C = K \times A/dl$$

where: K is the hydraulic conductivity
A is the cross-sectional area
dl is the distance between two nodes

For the mesh with 200 elements the ratio between the C value in y-direction and x-direction becomes 10^{+4} for the isotropic, homogeneous condition ($C_x = 0.3$, $C_y = 3,000$) and increases to 10^{+6} for the anisotropic, homogeneous condition ($C_x = 0.3$, $C_y = 300,000$). In comparison, the conductance value for an average element of the cross-sectional model (fig. 6) is $C_y/C_x = 2,420$ for isotropic conditions, and $C_y/C_x = 24.2$ for anisotropic conditions with $K_y/K_x = 0.01$.

The computed hydraulic heads at the corresponding node locations for the different simulations were compared and the differences in head, respectively, to the 4-element case are shown in figure A2. Additionally, the overall performance of the different simulations is listed in table A1. The 4-element case can be considered the true solution. The errors in computed hydraulic head are small and can be considered negligible for most practical purposes. Hence, the anisotropic node spacing in the present model does not cause significant numerical errors.

A comparison of steady-state hydraulic head distribution in the cross-sectional model computed by the program FREESURF and subsequent computation by FLUMPS showed good agreement of the results. This indicates that the effect of extreme node-spacing differences between horizontal and vertical directions in the model also does not produce a significant error when using the program FLUMPS.

DRAFT

FIGURE CAPTIONS

Figure 1. Plot of pressure-depth DST data from selected wells in the Deep-Basin Brine aquifer using high-quality class A data (initial and final shut-in pressure agree within 10%) (from Orr and Kreitler, 1985).

Figure 2. Fluid pressure changes as a result of (a) epeirogenetic movement, (b) erosion and deposition (after Bradely, 1975).

Figure 3. Fluid pressure changes as a result of erosional unloading with pore volume expansion of shale (after Ferran, 1972).

Figure 4. Structural features of Texas Panhandle and adjacent areas (modified from Handford, 1980).

Figure 5. Regional east-west cross section illustrating spatial relationships of the major depositional systems in the Palo Duro Basin (after Bassett and others, 1981).

Figure 6. Potentiometric surface map of the unconfined aquifers that overlie the evaporite sequences (after Bassett and others, 1981).

Figure 7. Potentiometric surface map of the Deep-Basin Brine aquifer constructed from kriged estimates of hydraulic head (after Wirojanagud and others, 1985).

Figure 8. Difference in hydraulic heads between unconfined aquifer and Deep-Basin Brine aquifer.

Figure 9. Finite element mesh representing the major hydrologic units. Each element is assigned a hydraulic conductivity value according to the different simulations. Numbered labels on the elements corespond to geologic facies listed in table 4. The upper surface of the mesh is represented with prescribed head boundary conditions and prescribed flux boundary conditions (High Plains surface) and represents the water-table. Heads are assumed to be uniform with depth along the eastern boundary. The lower surface of the mesh is a no-flow boundary which corresponds to the contact between the Deep-Basin Brine aquifer and basement rock.

Figure 10. Pressure-depth data from the Deep-Basin Brine aquifer, Jackson County, Oklahoma, which is located approximately at the eastern edge of the cross section. The pressure-depth regression line has a slope equivalent to brine hydrostatic.

Figure 11. Flow net from Simulation A-1 with hydraulic conductivities from table 4. Hydraulic heads beneath the Evaporite aquitard are lower by up to 300 m (1,000 ft) than unconfined heads. East of the Caprock Escarpment, however, hydraulic heads in the Deep-Basin Brine aquifer are unrealistically high.

Figure 12. Flow net from Simulation A-2 with increased permeability of proximal granite wash. It shows that subhydrostatic conditions prevail in the Deep-Basin Brine aquifer east of the escarpment.

1

DRAFT

Figure 13. Isolith map of Pennsylvanian and Wolfcampian granite wash in the Texas Panhandle (after Dutton and others, 1982).

Figure 14. Flow net from Simulation A-3 with increased hydraulic conductivities for granite wash compared to Simulation A-2. Depressuring is increased toward the western part of the Deep-Basin Brine aquifer. Ground-water flow within the Deep-Basin Brine aquifer is governed primarily by the spatial distribution of relatively permeable granite-wash deposits.

Figure 15. Flow net from Simulation B-1 with increased vertical permeability of the Evaporite aquitard. Hydraulic head increases drastically in the deep section.

Figure 16. Flow net from Simulation B-2 indicating a relatively small decrease in hydraulic heads in the deep section. In the San Andres unit 4 carbonate, a significant lateral flow component is shown.

Figure 17. Flow net from Simulation B-3 with decreased vertical permeability of the Evaporite aquitard. Hydraulic heads in the Deep-Basin Brine aquifer decrease by up to 50 m (164 ft) in the central part of the cross section.

Figure 18. Flow net from Simulation C considering decreased vertical permeability within the shallow aquifer system. Hydraulic heads in the deep section are not significantly changed compared to heads in Simulation A-2. Vertical leakage through the Evaporite aquitard, however, is reduced by about 19 percent.

Figure 19. Flow net from Simulation D with modified finite element mesh. Hydraulic heads increase in the western part of the cross section. In the eastern part, however, extensive subhydrostatic conditions are maintained. Ground-water flow into the Deep-Basin Brine aquifer increased from 0.0034 (Simulation A-2) to 0.047 m^3/day.

Figure 20. Hydraulic head distribution from Simulation T-1 with hydraulic conductivities from Table 2. Hydraulic head distribution represents the hypothetical pre-uplift hydrodynamic conditions assuming an overall hydraulic gradient across the surface of the model of 100 m.

Figure 21. Hydraulic head distribution from Simulation T-2 representing hydrodynamic conditions 10 million years after the beginning of the uplift event. During the first million years, hydraulic heads at the surface nodes were gradually increased by up to 1,100 m (3,600 ft) for the westernmost node relative to the heads along the eastern boundary which were kept constant. Initial conditions represent the results from Simulation T-1.

Figure 22. Flow net from the steady-state simulation equivalent to Simulation T-2. The assigned hydraulic heads along the upper surface of the mesh are the ultimate boundary conditions of Simulation T-2, representing the uplifted topographic surface.

Figure 23. Hydraulic head distribution from Simulation T-3 representing hydrodynamic conditions 10 million years after the beginning of Ogallala deposition. During the first million years, hydraulic heads at the surface nodes were gradually increased by up to 130 m (430 ft). Prescribed hydraulic heads along the High Plains surface were set equal to heads computed in Simulation A-2 (Senger and Fogg, 1984). Initial conditions are the computed heads from Simulation T-2.

2

Figure 24. Hydraulic head distribution from Simulation T-4 representing hydrodynamic conditions 5 million years after the onset of the Pecos valley erosion. Hydraulic heads at the boundary nodes of the area were gradually reduced during the first 4 million years to a level corresponding to the approximate valley topography. Initial conditions are the computed heads from Simulation T-3.

Figure 25. Difference in hydraulic heads before and after Pecos River erosion.

Figure 26. Hydraulic head distribution from Simulation T-5 representing hydrodynamic conditions 1.1 million years after the gradual retreat (18 cm/yr) of the Caprock Escarpment starting at the eastern boundary of the model. Initial conditions are the computed heads from Simulation T-4.

Figure 27. Difference in hydraulic head before and after cap-rock retreat.

Figure 28. Hydraulic head distribution from Simulation P-1 showing possible effects of erosional unloading conditions 800,000 years after gradual retreat (18 cm/yr) of the Caprock Escarpment from the eastern boundary of the model. The unloading causes local, temporary underpressuring beneath the Caprock Escarpment.

Figure 29. Hydraulic head distribution from Simulation H-1 showing effects of local hydrocarbon production in the Lower Permian strata 100 years after beginning of production.

3

DRAFT

APPENDIX FIGURES

Figure A1. Simplified model to test the effect of node spacing differences in horizontal and vertical direction.

Figure A2. Diagram showing the differences in computed hydraulic heads at the corresponding node locations with respect to the 4-element case.

TABLE CAPTIONS

Table 1. Generalized stratigraphic column of the Palo Duro Basin (modified from Bassett and Bentley, 1983).

Table 2. Permeability of individual hydrogeologic units of the Palo Duro Basin (after Wirojanagud and others, 1985).

Table 3. Summary of numerical simulations of the cross-sectional ground-water flow model: steady-state modeling.

Table 4. Assigned hydraulic conductivity values for the major hydrologic systems.

Table 5. Summary of numerical simulations of the cross-sectional ground-water flow model: transient modeling.

APPENDIX TABLE

Table A1. Performance of the simplified model at different conductance ratios.

1

DRAFT

Table 1. Generalized stratigraphic column of the Palo Duro Basin (modified from Bassett and Bentley, 1983).

System	Series	Group	General lithology and depositional setting	Hydrogeologic element	Hydrogeologic unit
Quaternary			Fluvial and lacustrine clastics		
Tertiary				Ogallala aquifer	Shallow aquifer
Cretaceous			Nearshore marine clastics		
Triassic		Dockum	Fluvial deltaic and lacustrine clastics and limestones	Dockum aquifer	
Permian	Ochoa		Salt, anhydrite, red beds and peritidal dolomite		
	Guadalupe	Artesia			
	Guadalupe	Pease River		Evaporite aquitard	Evaporite aquitard
	Leonard	Clear Fork			
	Leonard	Wichita			
	Wolfcamp			Wolfcamp carbonate aquifer	Wolfcamp carbonate
Pennsylvanian			Shelf and platform carbonates, basin shale and deltaic sandstones	Pennsylvanian carbonate aquifer	Deep-Basin Brine aquifer — Wolfcamp granite wash
			Basin shale	Upper Paleozoic granite wash aquifer	Basin shale
					Pennsylvanian carbonate
Mississippian			Shelf limestone and chert	Lower Paleozoic carbonate aquifer	Pennsylvanian granite wash
Ordovician		Ellenburger	Shelf dolomite		
Cambrian			Shallow marine (?) sandstone	Lower Paleozoic sandstone aquifer	Pre-Pennsylvanian-age rock
	Precambrian		Igneous and metamorphic	Basement aquiclude	Basement aquiclude

Table 2. Permeability of individual hydrogeologic units of Permian and Pennsylvanian of the Palo Duro Basin (after Wirojanagud and others, 1985).

	Hydrogeologic unit	Geometric mean of k $(e^{\bar{y}})$, md	Variance, s^2 [ln(K)]	Number and source of data	Typical value md
	Evaporite strata	——	——	——	.00028[++] (vertical permeability)
Deep brine aquifer	Wolfcampian carbonate	8.90	5.08	25 - DST data 70 - Core Lab Inc. (1972) 6 - Sawyer #1 pumping test data	
	Pennsylvanian carbonate	17.90	5.61	25 - DST data 118 - Core Lab Inc. (1972)	.07——300*
	shale	——	——	——	.0001 + .00001——.08*
	granite wash	8.60	7.13	10 - DST data 10 - Sawyer #1 pumping test 11 - Core Lab Inc. (1972)	.01——380*
	Pre-Pennsylvanian rock	4.76	5.70	11 - DST data 14 - Sawyer #1 pumping test data	——

*range of permeability, from Davis and DeWiest (1966), Davis (1980), Freeze and Cherry (1979)
+average permeability, assigned to basinal system (fig. 4)

++derived from the harmonic means of permeabilities using typical or measured values of permeability for each substrata

Table 3. Summary of steady-state simulations of the cross-sectional ground-water flow model.

Conditions	A1	A2	A3	B1	B2	B3	D	C
1. Granite Wash (GW) Permeability:								
uniform GW: k = 8.6 md	X							
distal GW: k = 8.6 md proximal GW: k = 100 md (east of escarpment)		X		X	X		X	X
distal GW: k = 100 md (extended into NM) proximal GW: k = 250 md (east of escarpment)			X					
2. Role of Evaporite Aquitard								
$k = 2.8 \times 10^{-3}$ md				X				
$k = 2.8 \times 10^{-4}$ md	X	X	X				X	X
$k = 2.8 \times 10^{-5}$ md					X			
$k = 2.8 \times 10^{-6}$ md						X		
3. Hydraulic Interconnection of Ogallala and Dockum								
Ogallala/Dockum aquifer: $K_x/K_z = 10$	X	X	X	X	X		X	
Ogallala aquifer: $K_x/K_z = 100$							X	
Dockum aquifer: $K_x/K_z = 10{,}000$							X	
4. Effect of Pecos River								X

Table 4. Assigned hydraulic conductivity values for the major hydrologic systems.

| Hydrologic Unit | Hydraulic Conductivity (m/day) | | Specific Storage[6] |
	horizontal (K_x)	vertical (K_z)	(m^{-1})
1. Ogallala fluvial system[1]	8.0×10^{0}	8.0×10^{-1}	10^{-4}
2. Triassic fluvial/lacustrine system[1]	8.0×10^{-1}	8.0×10^{-2}	10^{-4}
3. Permian (salt dissolution zone)[3]	8.2×10^{-2}	8.2×10^{-4}	10^{-4}
4. Permian sabkha system[4]	3.2×10^{-7}	3.2×10^{-7}	10^{-4}
5. Permian mud-flat system[2]	8.2×10^{-5}	8.2×10^{-5}	10^{-4}
6. Permian/Pennsylvanian shelf carbonates[4]	1.3×10^{-2}	1.3×10^{-4}	10^{-4}
7. Permian/Pennsylvanian basinal systems[4]	1.1×10^{-7}	1.0×10^{-7}	10^{-4}
8. Permian/Pennsylvanian mud-flat and alluvial/fan delta system[2]	8.2×10^{-2}	8.2×10^{-4}	10^{-4}
9. Permian/Pennsylvanian fan delta system (granite wash)[4]	$1.0 - 12.0 \times 10^{-2}$	$1.0 - 12.0 \times 10^{-4}$	10^{-4}
10. San Andres Cycle 5 dolomite[5]	1.2×10^{-4}	1.2×10^{-4}	10^{-4}

Sources of data:

1. K_x from Myers (1969); assumed $K_x/K_z = 10$

2. typical value of geologic material (Freeze and Cherry, 1979)

3. K_x from U.S. Geological Survey open-file data; assumed $K_x/K_z = 100$

4. after Wirojanagud and others (1985)

5. after Dutton (1983)

6. after Tóth and Millar (1983)

Table 5. Summary of simulations representing the different tectonic and geomorphologic events.

Simulation	Event/Process	Geologic Time Period	Simulated Time Period	Boundary Conditions	Hydrodynamic Conditions at the End of Simulation
T-1	Pre-Uplift	Prior to 15 m.y.	w.a.	Prescribed heads along the surface ranging from 600 m in the east to 700 m in the west	Steady-state
T-2	Uplift and Tilting	~15 m.y. to ?	10 m.y.	Increase prescribed heads along the surface from 0 m at the east to 1,100 m at the west during first 1 m.y.	Approximate steady-state
T-3	Deposition of Ogallala	~13 m.y. to ~3 m.y.	10 m.y.	Increase prescribed heads along the surface from 50 m in the east to 130 m in the west during first 1 m.y.	Approximate steady-state
T-4	Erosion of the Pecos River Valley	Within the last 5 m.y.	5 m.y.	Decrease of prescribed heads along the Pecos valley by up to 325 m during the first 4 m.y.	Overall steady-state
T-5	Westward Retreat of Caprock	Within the last 3 m.y.	1.1 m.y.	Decrease of prescribed heads along the present-day Rolling Plains surface corresponding to rate of caprock retreat of 18 cm/yr	Local transient conditions
P-1	Effect of Erosional Decompaction during Caprock Retreat	Within the last 1 m.y.	800,000 yrs.	Decrease of prescribed heads along the present-day Rolling Plains surface corresponding to a rate of cap-rock retreat of 18 cm/yr. In addition, assume decompaction for the shallow aquitard unit underlying the Rolling Plains	Local transient conditions
H-1	Effect of Hydro-carbon Production	Within the last 60 yrs.	100 yrs.	Decrease prescribed heads of two node locations by 200 m during the first 50 yrs.	Local transient conditions

DRAFT

Table A1. Performance of the model at different conductance ratios.

1. isotropic system: $K_x = K_y = 30$ m/day

	Total discharge (#7)	Mass Balance (%)*	Conductance Ratio C_y/C_x
4 elements	887.8049	$-.123 \times 10^{-11}$	4
50 elements	844.4009	$-.162 \times 10^{-9}$	625
100 elements	844.1807	$+.149 \times 10^{-7}$	2,500
200 elements	844.1807	$-.149 \times 10^{-7}$	10,000

2. anisotropic: $K_x = 30$ m/day $K_y = 3,000$ m/day

	Total discharge (#7)	Mass Balance (%)*	Conductance Ratio C_y/C_x
4 elements	1486.432	$-.266 \times 10^{-9}$	400
50 elements	1485.612	$-.241 \times 10^{-6}$	62,500
100 elements	1485.609	$.160 \times 10^{-6}$	250,000
200 elements	1485.607	$-.357 \times 10^{-5}$	1,000,000

*Mass balance $= \dfrac{(\text{inflow} - \text{outflow})}{\text{inflow}} \times 100$
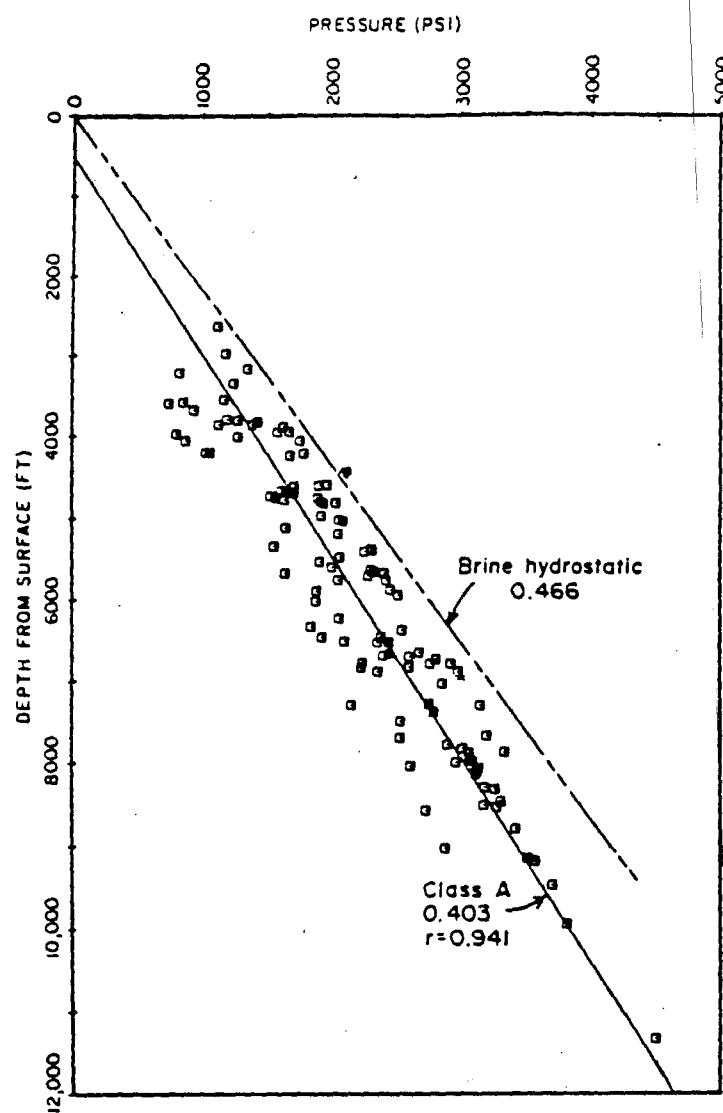
Figure 1. Plot of pressure-depth DST data from selected wells in the Deep-Basin Brine aquifer using high-quality class A data (initial and final shut-in pressure agree within 10%) (from Orr and Kreitler, 1985).

DRAFT
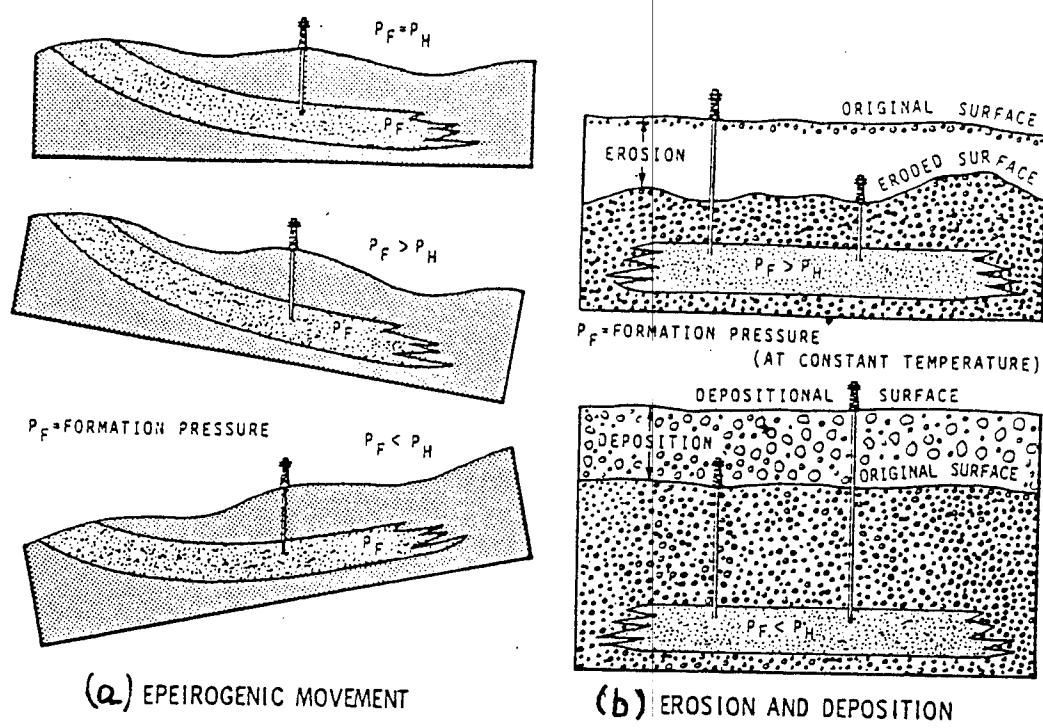
(a) EPEIROGENIC MOVEMENT

(b) EROSION AND DEPOSITION

Figure 2. Fluid pressure changes as a result of (a) epeirogenetic movement, (b) erosion and deposition (after Bradely, 1975).
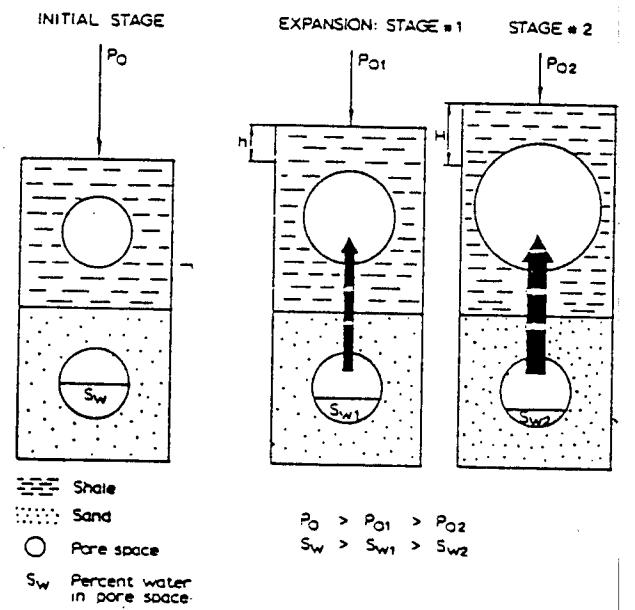
c.) Overburden pressure Reduction

Figure 3. Fluid pressure changes as a result of erosional unloading with pore volume expansion of shale (after Ferran, 1972).

Figure 4. Structural features of Texas Panhandle and adjacent areas (modified from Handford, 1980).

West

East

NEW MEXICO | TEXAS

TEXAS | OKLAHOMA

PECOS RIVER

FLUVIAL SYSTEM (OGALLALA)

MUDFLAT & ALLUVIAL/FAN-DELTA SYSTEMS

FLUVIAL & LACUSTRINE SYSTEMS (DOCKUM)

COASTAL SABKHA & SALT PAN SYSTEMS

INNER SHELF & COASTAL SABKHA SYSTEMS

PRAIRIE DOG TOWN FORK

SALT-DISSOLUTION ZONE

MUDFLAT SYSTEM

Sea level

COASTAL SABKHA & SALT PAN SYSTEMS

Sea level

SHELF & SHELF-MARGIN SYSTEMS

INNER SHELF & COASTAL SABKHA SYSTEMS

BASIN SYSTEM

FAN-DELTA SYSTEM

CRYSTALLINE BASEMENT

N M

TEXAS

OK

AMARILLO UPLIFT

PALO DURO BASIN

LINE OF SECTION

MATADOR ARCH

m ft
300 800

0   0

20mi

30km

QA1078
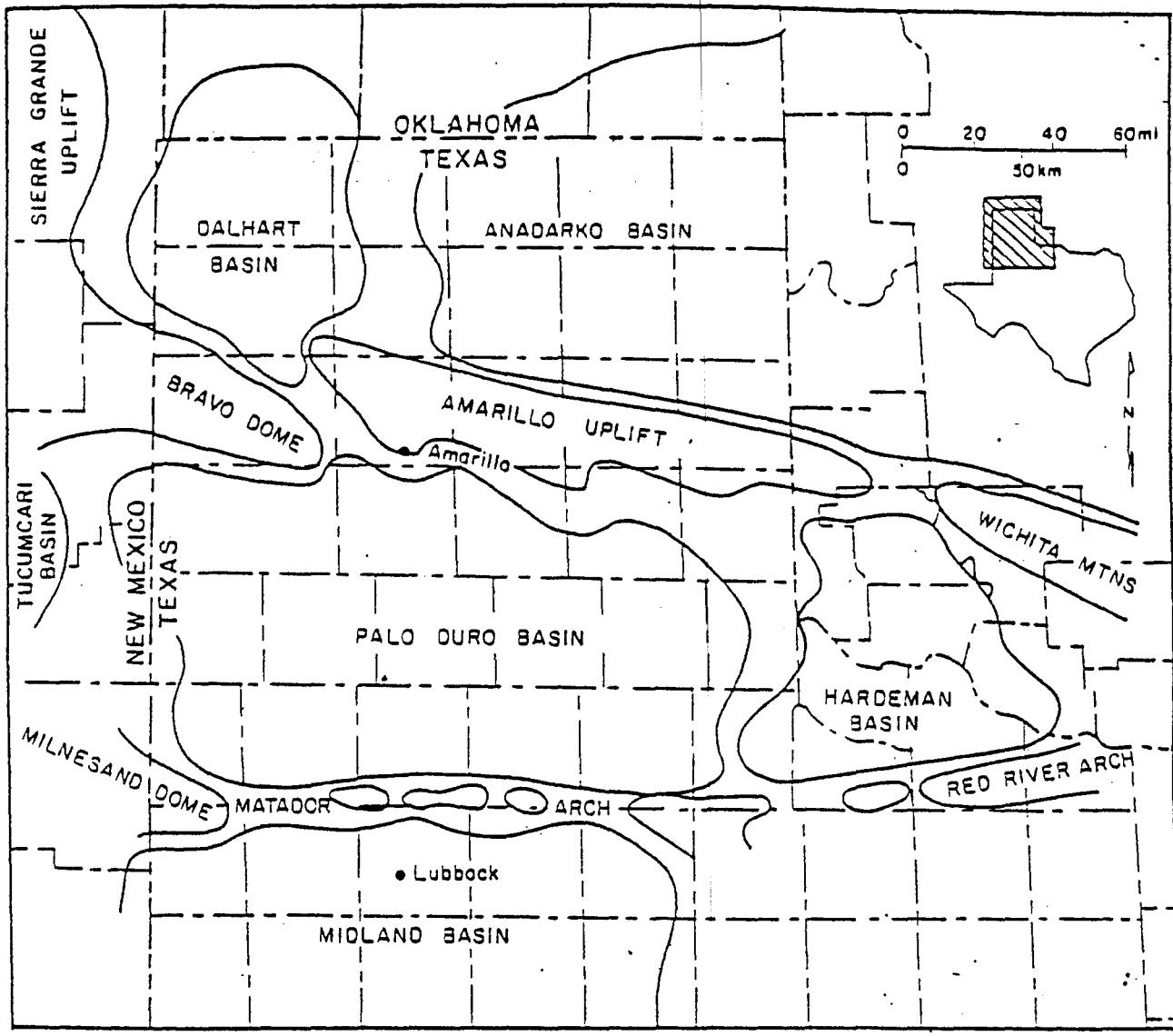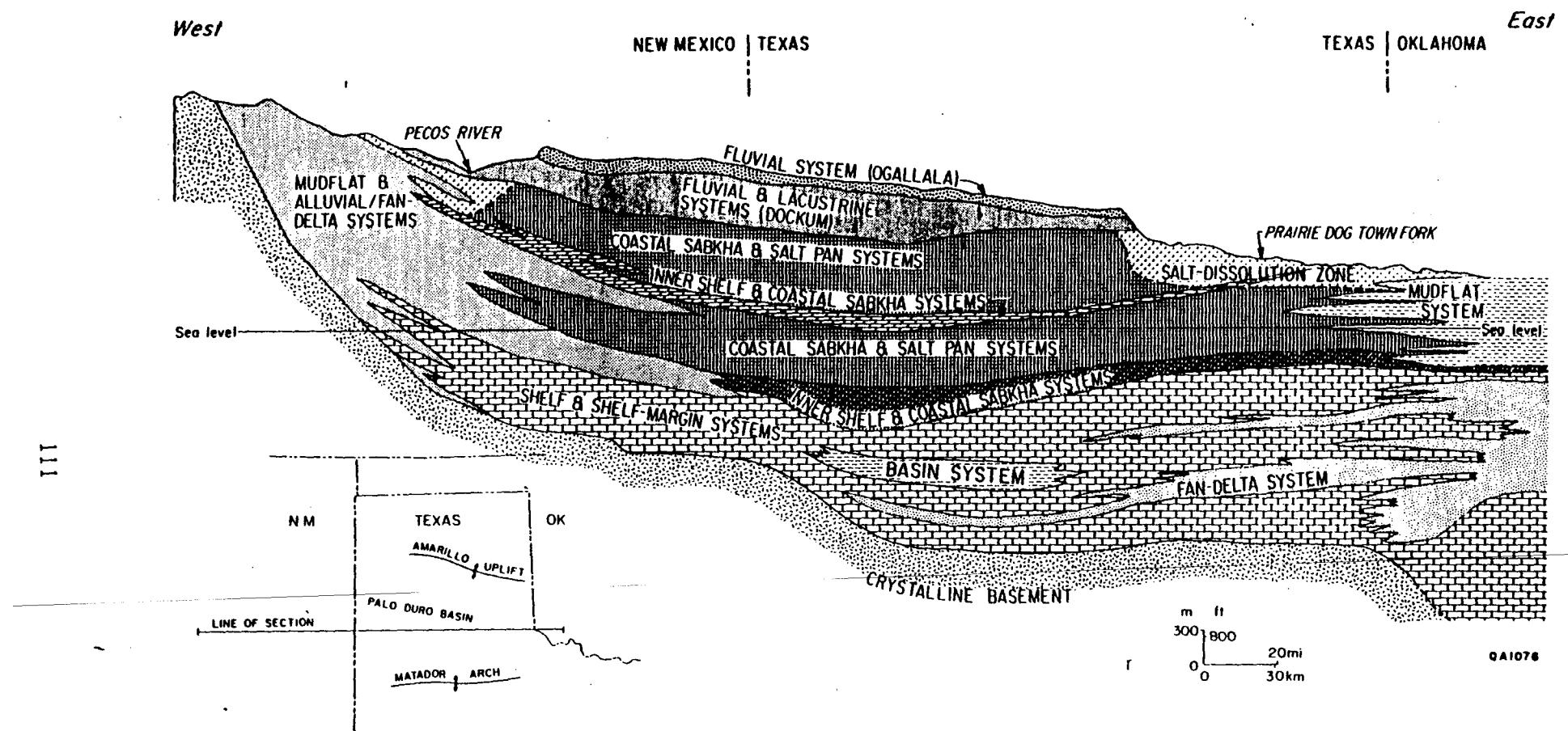
Figure 5. Regional east-west cross section through eastern New Mexico and the Texas Panhandle illustrating stratigraphic relations of the major depositional systems in the Palo Duro Basin.

Figure 6. Potentiometric surface map of the unconfined aquifers that overlie the evaporite sequences (after Bassett and others, 1981).

Figure 7. Potentiometric surface map of the Deep-Basin Brine aquifer constructed from kriged estimates of hydraulic head (after Wirojanagud and others, 1985).

CONTOURS OF HEAD DIFFERENCE, OGALLALA-DEEP-BRINE AQUIFER

--- Cross-sectional Traverse

Figure 8. Difference in hydraulic heads between unconfined aquifer and Deep-Basin Brine aquifer.

West

NEW MEXICO | TEXAS   East | OKLAHOMA

EXPLANATION

▓▓ Ogallala fluvial system

▓▓ Triassic fluvial/lacustrine system

▓▓ Permian (salt dissolution zone)

▓▓ Permian sabkha system

▓▓ Permian mud-flat system

▓▓ Permian/Pennsylvanian shelf carbonates

▓▓ Permian/Pennsylvanian basinal systems

▢ Permian/Pennsylvanian mud-flat and alluvial/fan delta system

▓ Permian/Pennsylvanian fan delta system (granite wash)

▢ San Andres Cycle 5 dolomite

Pecos River Valley   High Plains Surface

OGALLALA

DOCKUM

Sea level — —

EVAPORITE AQUITARD

— — Sea level

DEEP BASIN
BRINE AQUIFER

SCALE

m   ft

900 ┌ 2400

300 └ 800   20   40 mi

0   30   60 km

NM   TEXAS   OK

Amarillo Uplift

Palo Duro Basin

Line of Section

Matador Arch

QA5048

Figure 9. Finite element mesh representing the major hydrologic units. Each element is assigned a hydraulic conductivity value according to the different simulations. Numbered labels on the elements corespond to geologic facies listed in table 4. The upper surface of the mesh is represented with prescribed head boundary conditions and prescribed flux boundary conditions (High Plains surface) and represents the water-table. Heads are assumed to be uniform with depth along the eastern boundary. The lower surface of the mesh is a no-flow boundary which corresponds to the contact between the Deep-Basin Brine aquifer and basement rock.

JACKSON COUNTY

Figure 10. Pressure-depth data from the Deep-Basin Brine aquifer, Jackson County, Oklahoma, which is located approximately at the eastern edge of the cross section. The pressure-depth regression line has a slope equivalent to brine hydrostatic.

Figure 11. Flow net from Simulation A-1 with hydraulic conductivities from table 4. Hydraulic heads beneath the Evaporite aquitard are lower by up to 300 m (1,000 ft) than unconfined heads. East of the Caprock Escarpment, however, hydraulic heads in the Deep-Basin Brine aquifer are unrealistically high.

EXPLANATION

——900—— Equipotential
(m above mean sea level)

——————➤ Streamline

Streamline contour interval:

| ░░░░░░ | 0.2 m³/d |

| ☐ | 0.01 m³/d |

---------- Formation boundary

Contour interval 50 m

Figure 12. Flow net from Simulation A-2 with increased permeability of proximal granite wash. It shows that subhydrostatic conditions prevail in the Deep-Basin Brine aquifer east of the escarpment.

Figure 13. Isolith map of Pennsylvanian and Wolfcampian granite wash in the Texas Panhandle (after Dutton and others, 1982).

EXPLANATION

——900—— Equipotential
(m above mean sea level)

———→ Streamline

Streamline contour interval:

░░░░ 0.2 m³/d

▢ 0.01 m³/d

---------- Formation boundary

Contour interval 50 m

Figure 14. Flow net from Simulation A-3 with increased hydraulic conductivities for granite wash compared to Simulation A-2. Depressuring is increased toward the western part of the Deep-Basin Brine aquifer. Ground-water flow within the Deep-Basin Brine aquifer is governed primarily by the spatial distribution of relatively permeable granite-wash deposits.

EXPLANATION

———900——— Equipotential
(m above mean sea level)

————▶ Streamline

Streamline contour Interval:

▨ 0.2 m³/d

▭ 0.01 m³/d

---------- Formation boundary

Contour interval 50 m

Figure 15. Flow net from Simulation B-1 with increased vertical permeability of the Evaporite aquitard. Hydraulic head increases drastically in the deep section.

EXPLANATION

——900—— Equipotential
(m above mean sea level)

————→ Streamline

Streamline contour interval:

▨ 0.2 m³/d

☐ 0.01 m³/d

---------- Formation boundary

Contour interval   50 m

Figure 16. Flow net from Simulation B-2 indicating a relatively small decrease in hydraulic heads in the deep section. In the San Andres unit 4 carbonate, a significant lateral flow component is shown.

EXPLANATION

—900— Equipotential (m above mean sea level)

——→ Streamline

Streamline contour interval:

[shaded] 0.2 m³/d

[blank] 0.01 m³/d

--------- Formation boundary

Contour interval 50 m

QA 5055

Figure 17. Flow net from Simulation B-3 with decreased vertical permeability of the Evaporite aquitard. Hydraulic heads in the Deep-Basin Brine aquifer decrease by up to 50 m (164 ft) in the central part of the cross section.

EXPLANATION

——900—— Equipotential
(m above mean sea level)

———→ Streamline

Streamline contour interval:

▓▓▓ 0.2 m³/d

☐ 0.01 m³/d

------- Formation boundary

Contour interval 50 m

QA 5056

ft   m
5,000 ⊤ 1,500

                    50 mi
0 ┼   ┤
0   80 km

Figure 18. Flow net from Simulation C considering decreased vertical permeability within the shallow aquifer system. Hydraulic heads in the deep section are not significantly changed compared to heads in Simulation A-2. Vertical leakage through the Evaporite aquitard, however, is reduced by about 19 percent.

EXPLANATION

——900—— Equipotential
(m above mean sea level)

——————▶ Streamline

Streamline contour interval:

[shaded] 0.2 m³/d

[blank] 0.01 m³/d

---------- Formation boundary

Contour interval 50 m

QA 5050

Figure 19. Flow net from Simulation D with modified finite element mesh. Hydraulic heads increase in the western part of the cross section. In the eastern part, however, extensive subhydrostatic conditions are maintained. Ground-water flow into the Deep-Basin Brine aquifer increased from 0.0034 (Simulation A-2) to 0.047 m³/day.

N.M. | TX.
TX. | OKLA.

700 m
600 m

680
660
640
620

——— Hydraulic head contour
interval = 10 m

– – – Prescribed heads along the
surface of the mesh (m.ams)

Figure 20. Simulation T-1 of computed hydraulic head distribution with hydraulic conductivities from Table 2. Hydraulic head distribution represents the hypothetical pre-uplift hydrodynamic conditions assuming an overall hydraulic gradient across the surface of the model of 100 m.
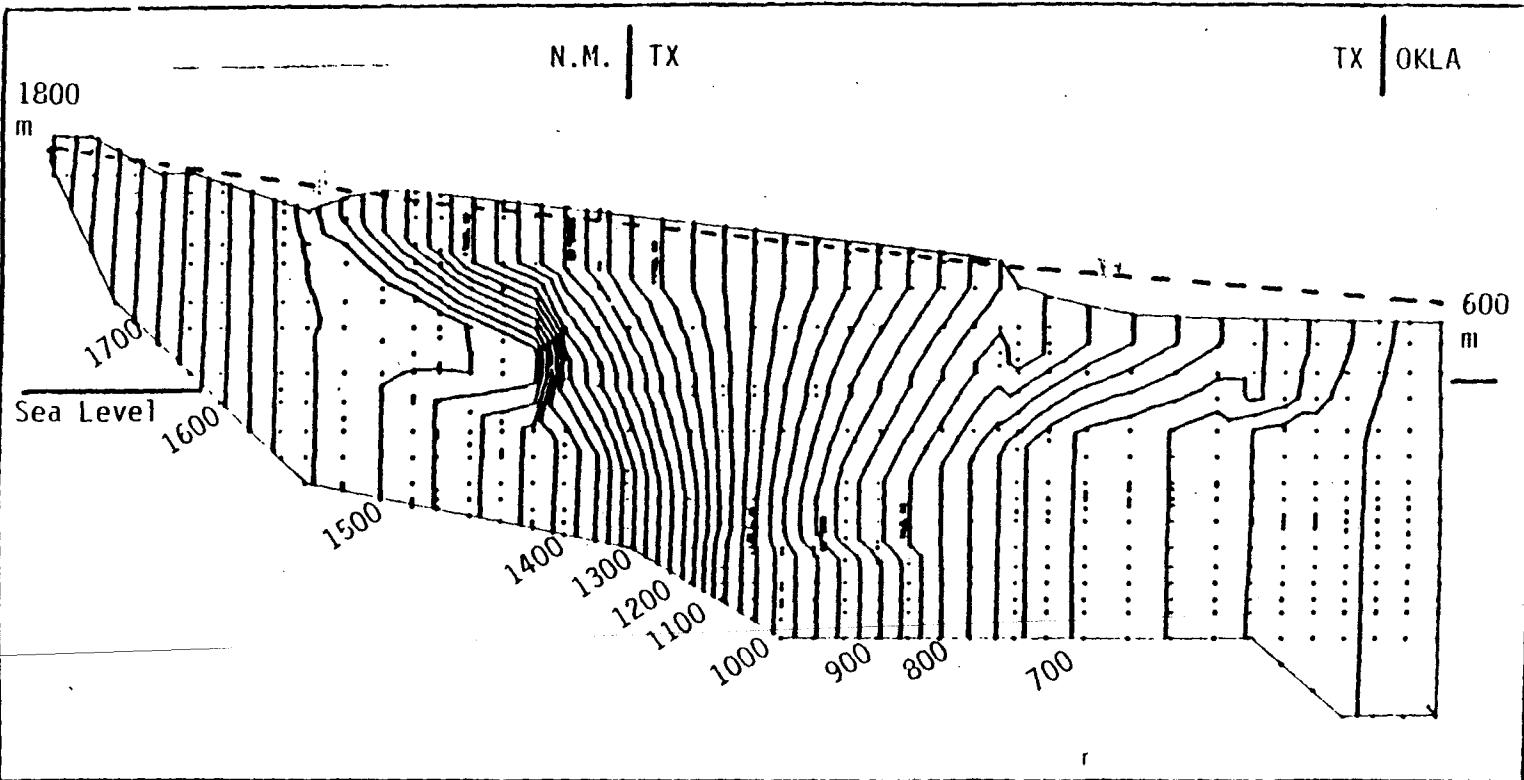
Figure 21. Simulation T-2 of computed hydraulic head distribution, representing hydrodynamic conditions 10 million years after the beginning of the uplift event. During the first million years, hydraulic heads at the surface nodes were gradually increased by up to 1,100 m (3,600 ft) for the westernmost node relative to the heads along the eastern boundary which were kept constant. Initial conditions represent the results from simulation T-1.
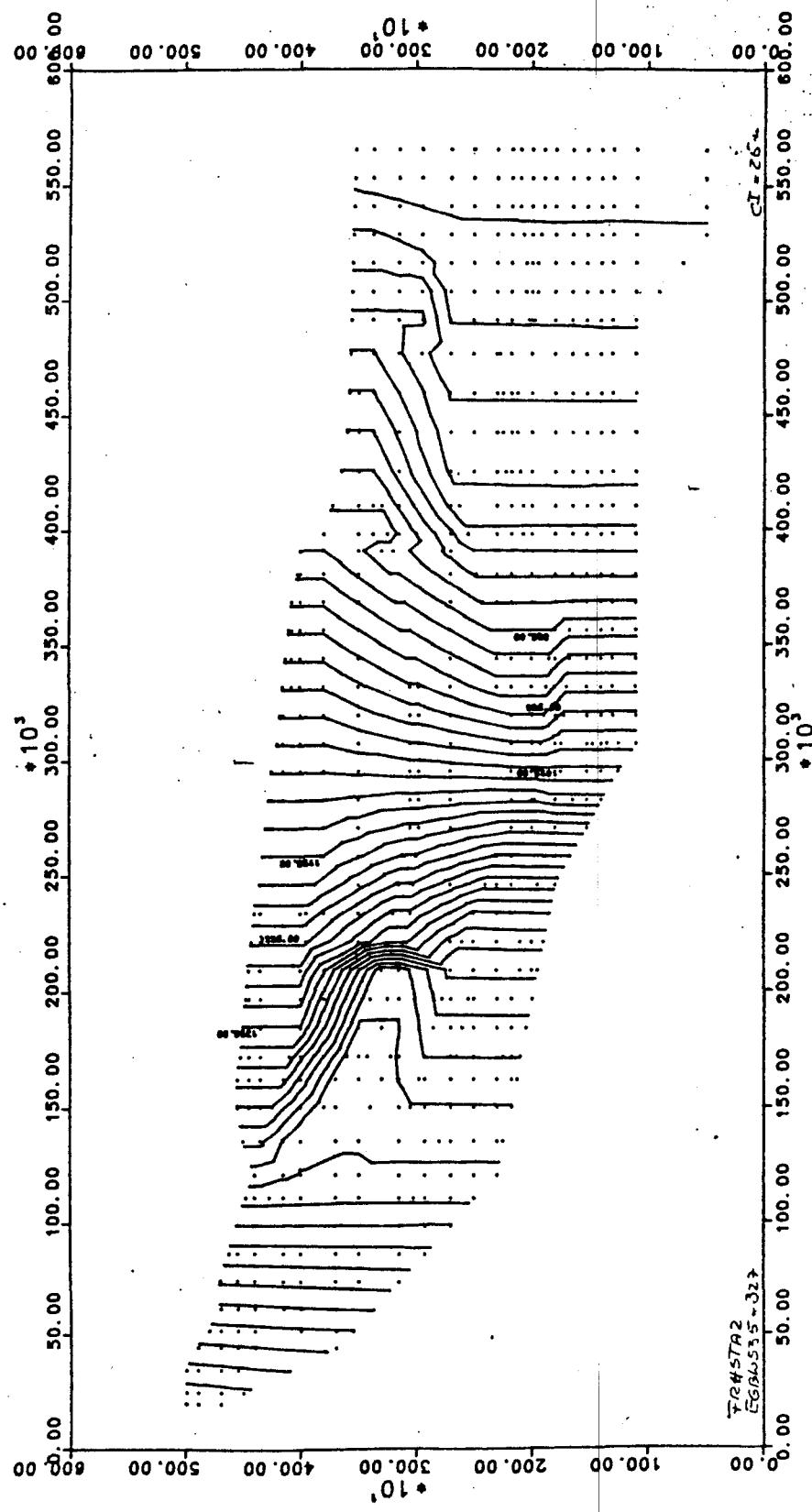
Fig. 22a. Hydraulic heads (steady-state simulation of T-2)

DRAFT
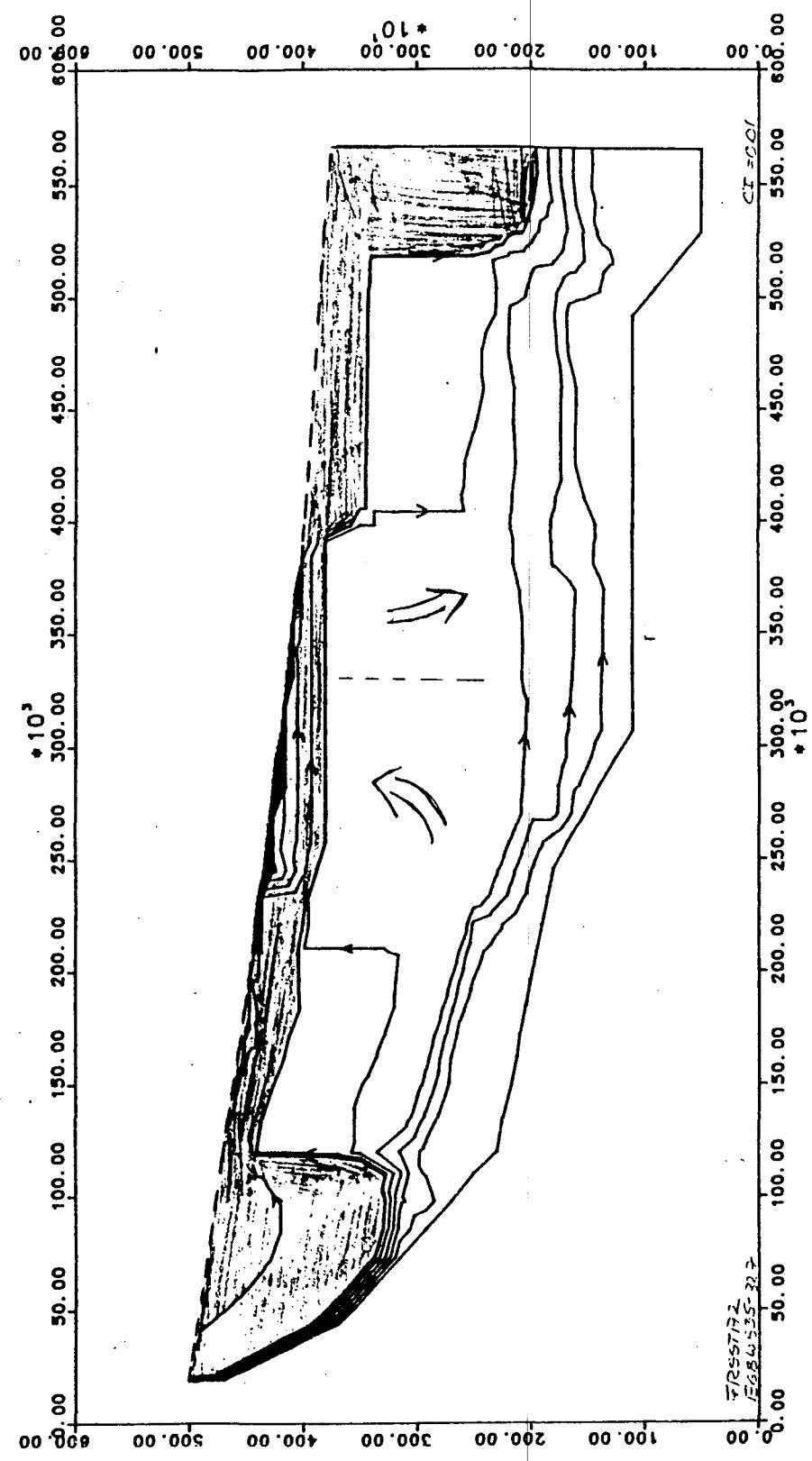
Fig. 22b. streamlines (steady state simulation of T-2)
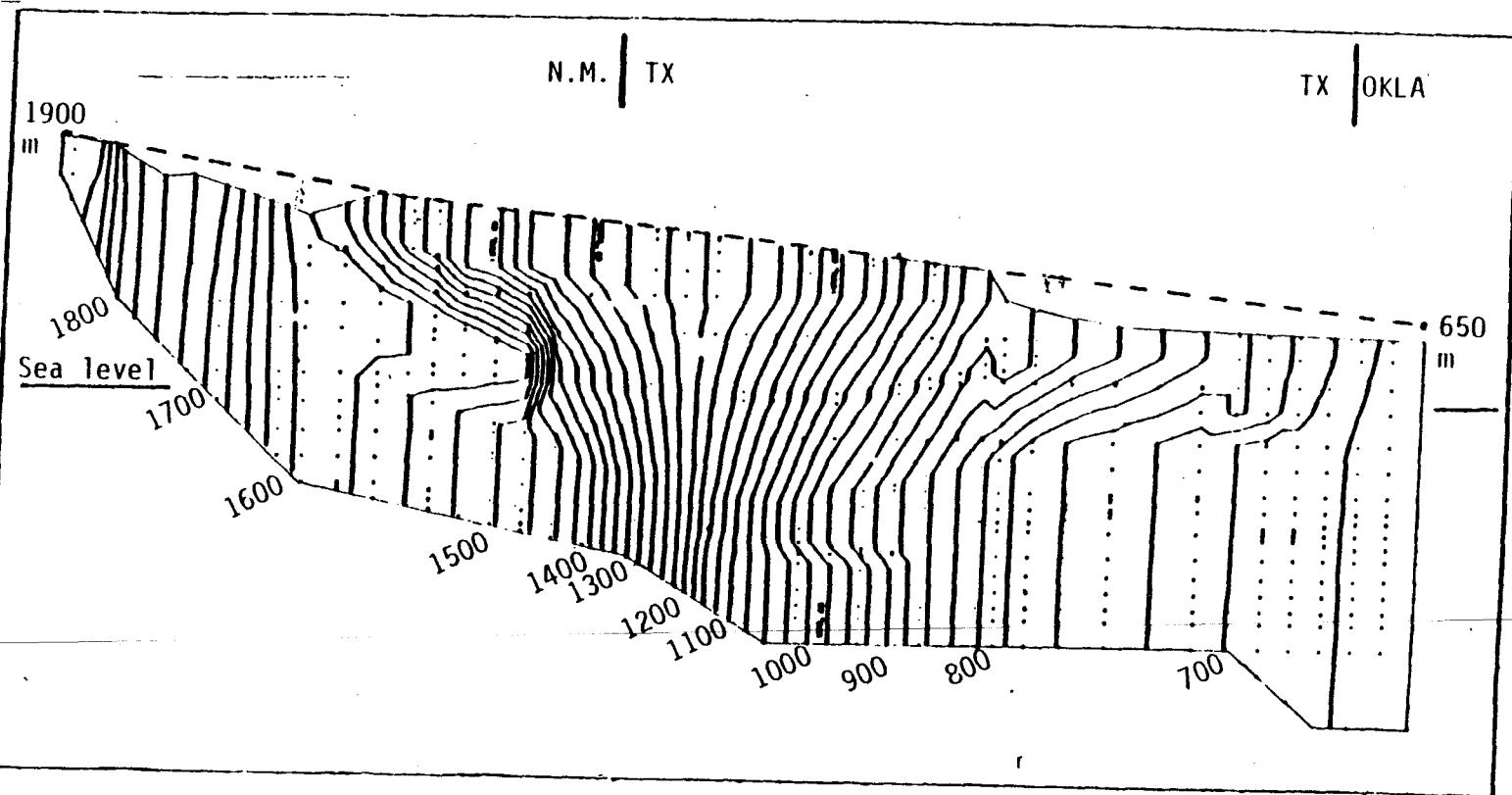
Figure 23. Simulation T-3 of computed hydraulic head distribution representing hydrodynamic conditions 10 million years after the beginning of Ogallala deposition. During the first million years, hydraulic heads at the surface nodes were gradually increased by up to 130 m (430 ft). Prescribed hydraulic heads along the High Plains surface were correlated with heads computed in simulation A-2. Initial conditions are the computed heads from simulation T-2.

Figure 24. Simulation T-4 of computed hydraulic head distribution representing hydrodynamic conditions 5 million years after the onset of the Pecos valley erosion. Hydraulic heads at the boundary nodes of the area were gradually reduced during the first 4 million years to a level corresponding to the approximate valley topography. Initial conditions are the computed heads from simulation T-3.

N.M. | TX   TX | OKLA

325 m

25
100
150
200
250

250
200
150
100   50   25

r

——— Hydraulic head difference
(negative) between simula-
tions T-3 and T-4.
Contour interval = 25 m

Figure 25. Difference in hydraulic heads before and after Pecos River erosion.

Figure 26. Simulation T-5 of computed hydraulic head distribution representing hydrodynamic conditions 1.1 million years after the gradual retreat (18 cm/yr) of the Caprock Escarpment starting at the eastern boundary of the model. Initial conditions are the computed heads from simulation T-4.

Figure 27. Difference in hydraulic head before and after Caprock retreat.

N.M. | TX

TX | OKLA

Sea
Level

300 250 200

25

150 200 250

——— Hydraulic head difference
(negative) between simula-
tions T-4 and T-5
Contour interval = 25 m

Figure 28. Hydraulic head distribution from Simulation P-1 showing possible effects of erosional unloading conditions 800,000 years after gradual retreat (18 cm/yr) of the Caprock Escarpment from the eastern boundary of the model. The unloading causes local, temporary underpressuring beneath the Caprock Escarpment.

N.M. | TX   TX | OKLA
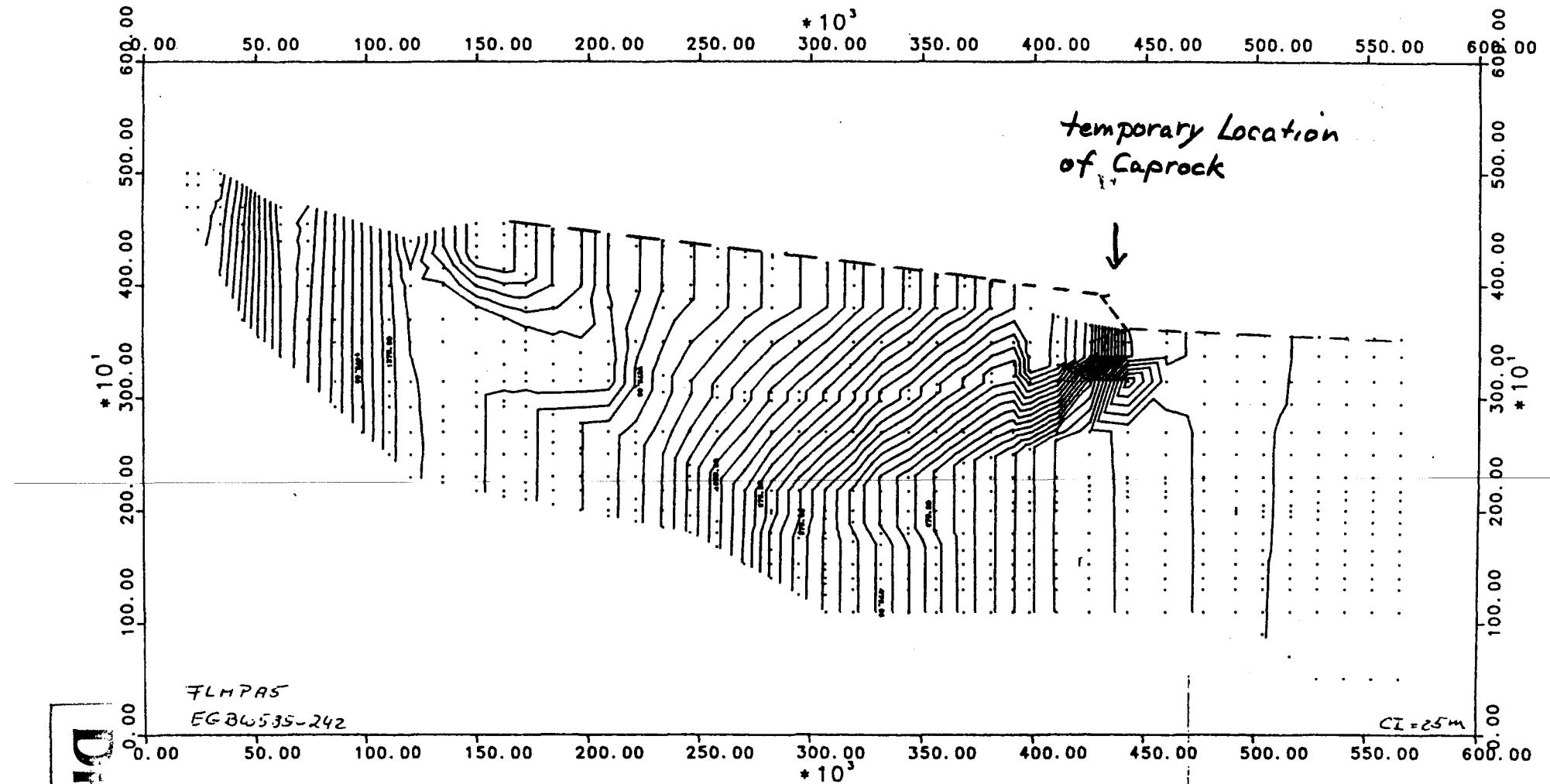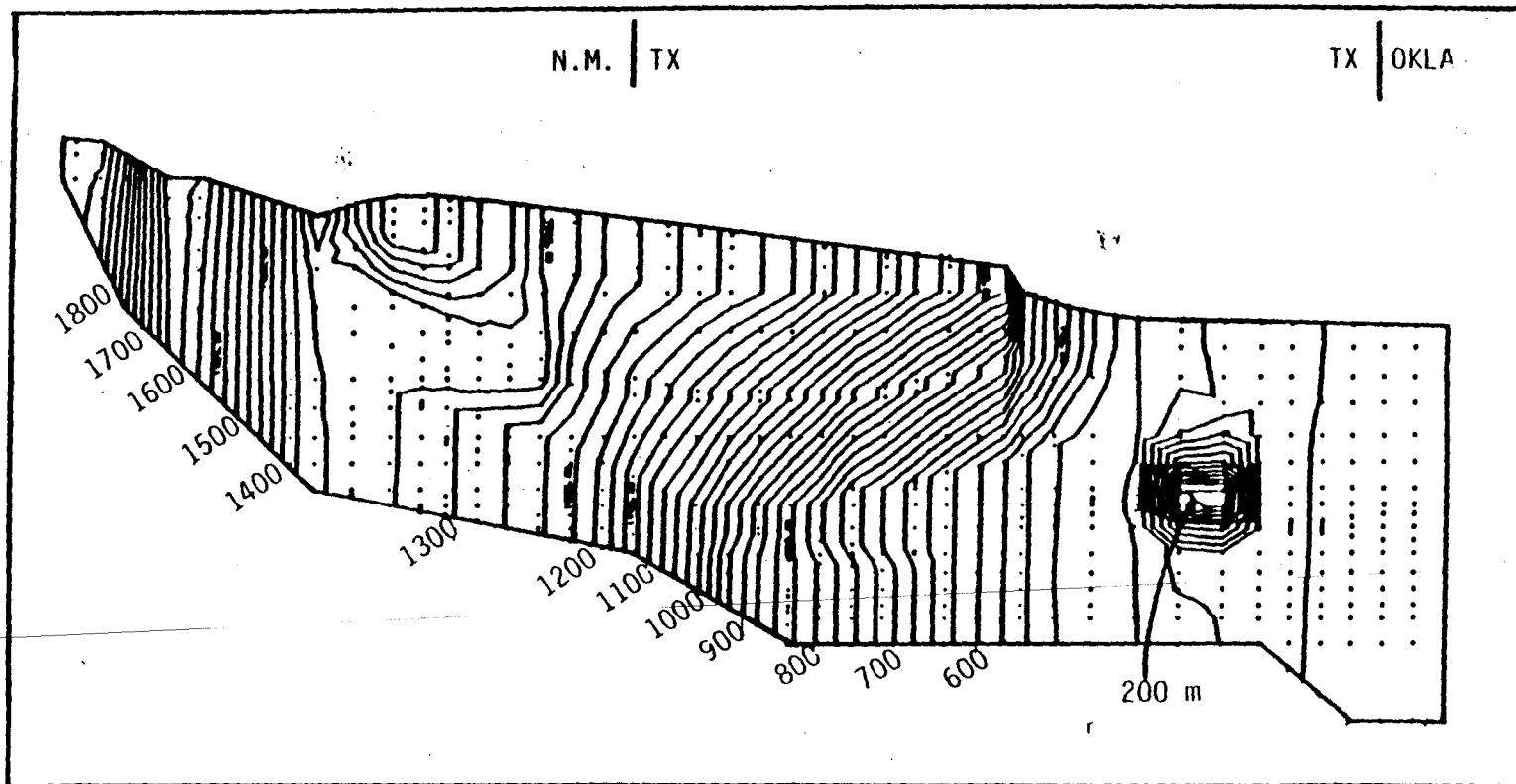
——— Hydraulic head contour
      interval = 25 m

— — — Prescribed heads along the
      surface of the mesh (m.ams)

Figure 29. Simulation H-1 of computed hydraulic head distribution representing the hydrodynamic conditions as a result of hydrocarbon production 100 years after the beginning of gradual reservoir pressure decline.
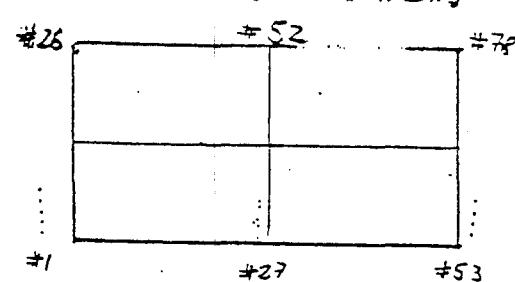
Figure A-1: A finite difference grid was set up with 4, 50, 100, and 200 elements with each mesh having the same total size. The finite difference mesh consists of three columns of nodes and is subdivided horizontally to obtain 4, 5, 100, or 200 elements.
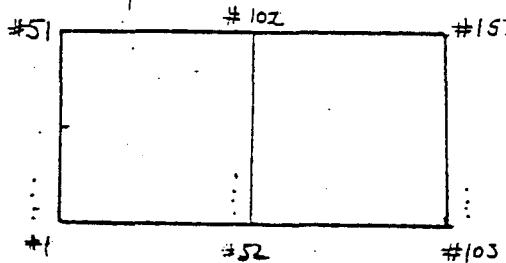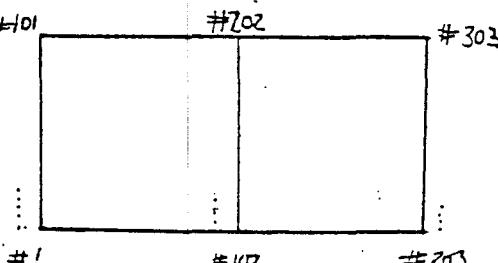
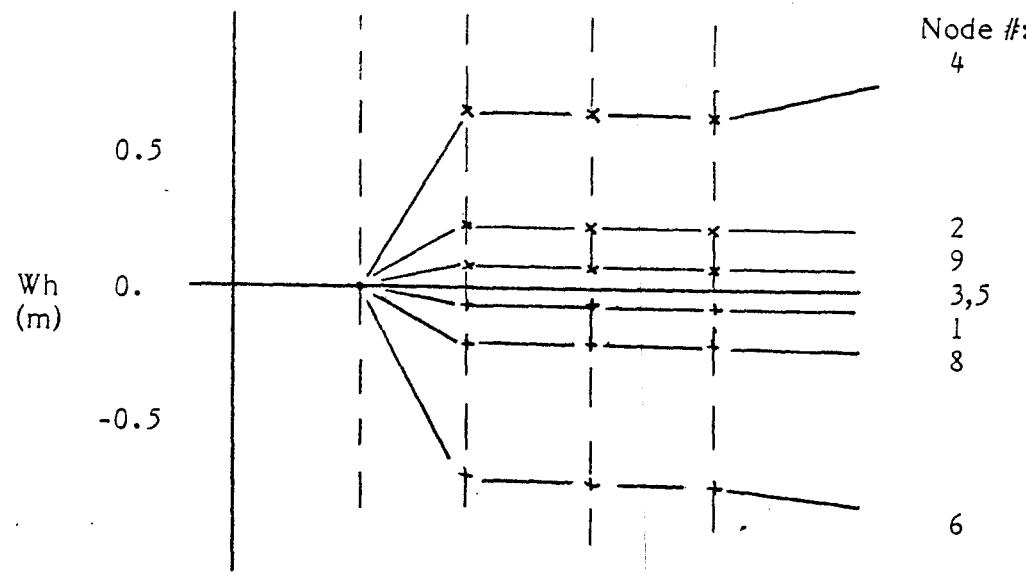1. 4 Elements
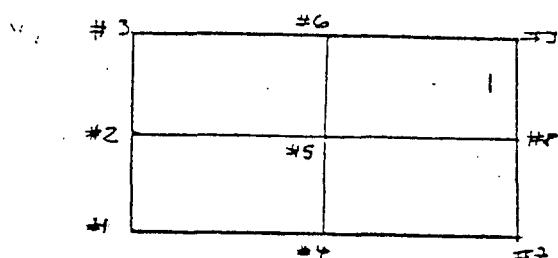
2. 50 Elements

3. 100 Elements

4. 200 Elements

DRAFT

Figure A2. Diagram showing the differences in computed hydraulic heads at the corresponding node locations with respect to the 4-element case.

a. isotropic homogeneous conditions

b. anisotropic homogeneous conditions

4 el.   50 el.   100 el.   200 el.